J. Plasma Phys. (2017), *vol.* 83, 705830301 © Cambridge University Press 2017 1
doi:10.1017/S0022377817000381

Electron inertia and quasi-neutrality in the Weibel instability

Enrico Camporeale[1,†] **and Cesare Tronci**[2]

[1]Center for Mathematics and Computer Science (CWI), 1098 XG Amsterdam, The Netherlands

[2]Department of Mathematics, University of Surrey, Guildford GU2 7XH, United Kingdom

Special issue contribution, on the occasion of the Vlasovia 2016 conference

(Received 29 December 2016; revised 8 May 2017; accepted 9 May 2017)

While electron kinetic effects are well known to be of fundamental importance in several situations, the electron mean-flow inertia is often neglected when length scales below the electron skin depth become irrelevant. This has led to the formulation of different reduced models, where electron inertia terms are discarded while retaining some or all kinetic effects. Upon considering general full-orbit particle trajectories, this paper compares the dispersion relations emerging from such models in the case of the Weibel instability. As a result, the question of how length scales below the electron skin depth can be neglected in a kinetic treatment emerges as an unsolved problem, since all current theories suffer from drawbacks of different nature. Alternatively, we discuss fully kinetic theories that remove all these drawbacks by restricting to frequencies well below the plasma frequency of both ions and electrons. By giving up on the length scale restrictions appearing in previous works, these models are obtained by assuming quasi-neutrality in the full Vlasov–Maxwell system.

Key words: plasma instabilities

1. Introduction: Ohm's law and electron inertia

Electron kinetic effects play a crucial role in a variety of situations. For example, the development of non-gyrotropic components in the electron pressure tensor is a well-known mechanism that drives collisionless magnetic reconnection (see, e.g. Camporeale & Lapenta 2005; Aunai, Hesse & Kuznetsova 2013; Haynes, Burgess & Camporeale 2014; Cazzola *et al.* 2016; Swisdak 2016). Indeed, the non-gyrotropic electron pressure is among the main mechanisms driving fast reconnection at length scales bigger than the plasma skin depth (also known as the *electron inertial length*). More specifically, collisionless reconnection is produced by the last two (non-ideal) terms in the electron momentum equation

$$q_e n_e \boldsymbol{E} = q_i n_i \boldsymbol{V}_i \times \boldsymbol{B} - \boldsymbol{J} \times \boldsymbol{B} + \nabla \cdot \widetilde{\mathbb{P}}_e + m_e n_e \frac{\mathrm{D}\boldsymbol{V}_e}{\mathrm{D}t}, \tag{1.1}$$

with the definitions (in standard notation)

$$n_k(\boldsymbol{x}, t) = \int f_k(\boldsymbol{x}, \boldsymbol{v}, t)\, \mathrm{d}\boldsymbol{v}, \tag{1.2}$$

† Email address for correspondence: e.camporeale@cwi.nl

$$\boldsymbol{V}_k(\boldsymbol{x},t)=n_k^{-1}\int f_k(\boldsymbol{x},\boldsymbol{v},t)\,\mathrm{d}\boldsymbol{v}, \tag{1.3}$$

$$\widetilde{\mathbb{P}}_k(\boldsymbol{x},t)=m_k\int(\boldsymbol{v}-\boldsymbol{V}_k)(\boldsymbol{v}-\boldsymbol{V}_k)f_k(\boldsymbol{x},\boldsymbol{v},t)\,\mathrm{d}\boldsymbol{v}. \tag{1.4}$$

Here, $f_k(\boldsymbol{x},\boldsymbol{v},t)$ is the phase-space density of the kth particle species ($k=i,e$ denotes the ions and the electrons, respectively) and $\mathrm{D}/\mathrm{D}t=\partial/\partial t+\boldsymbol{V}_e\boldsymbol{\cdot}\nabla$ is the convective derivative. Upon neglecting the displacement current (so that $\boldsymbol{J}=\mu_0^{-1}\nabla\times\boldsymbol{B}$) and by invoking quasi-neutrality (so that $n_i=-q_en_e/q_i$), one obtains the generalized Ohm's law in the form

$$\boldsymbol{E}=-\boldsymbol{V}_i\times\boldsymbol{B}-\frac{1}{\mu_0en_e}\boldsymbol{B}\times(\nabla\times\boldsymbol{B})-\frac{1}{en_e}\nabla\boldsymbol{\cdot}\widetilde{\mathbb{P}}_e-\frac{m_e}{e}\frac{\mathrm{D}\boldsymbol{V}_e}{\mathrm{D}t}, \tag{1.5}$$

where we have used the notation $q_i=Ze=-Zq_e$ for the ion and electron charges. Each term on the right-hand side of Ohm's law has been extensively studied in terms of its contribution to the reconnection flux (Cai & Lee 1997; Wang, Bhattacharjee & Ma 2000; Birn *et al.* 2001). The last term is associated with the inertia of the electron mean flow and this generates microscopic instabilities at the scale of the skin depth $\delta_e=c/\omega_{pe}$, which can then drive reconnection. However, these length scales are often neglected in reduced reconnection models by discarding the electron mean-flow inertia term, so that Ohm's law becomes

$$\boldsymbol{E}=-\boldsymbol{V}_i\times\boldsymbol{B}-\frac{1}{\mu_0en_e}\boldsymbol{B}\times(\nabla\times\boldsymbol{B})-\frac{1}{en_e}\nabla\boldsymbol{\cdot}\widetilde{\mathbb{P}}_e. \tag{1.6}$$

This reduced form of Ohm's law has been adopted in a variety of works (Hesse & Winske 1993, 1994; Winske & Hesse 1994; Kuznetsova, Hesse & Winske 1998, 2000; Yin *et al.* 2001; Yin & Winske 2003; Hesse, Kuznetsova & Birn 2004). In these works, equation (1.6) is combined with a moment truncation for the electron pressure dynamics, which is then coupled to ion motion in either fluid or kinetic description.

Cheng & Johnson (1999) followed a different strategy for obtaining a reduced model. While retaining small length scales, their approach neglected high frequencies by adopting the quasi-neutral limit of the Vlasov–Maxwell system. More specifically, using Ampère's law leads to rewriting (with no approximation) the generalized Ohm's law (1.5) as

$$\begin{aligned}\left(1+\frac{Zm_e}{m_i}\right)\boldsymbol{E}\;=\;&-\left(1+\frac{Zm_e}{m_i}\right)\boldsymbol{V}_i\times\boldsymbol{B}+\frac{1}{en_e}\left[\boldsymbol{J}\times\boldsymbol{B}-\nabla\boldsymbol{\cdot}\left(\widetilde{\mathbb{P}}_e-\frac{Zm_e}{m_i}\widetilde{\mathbb{P}}_i\right)\right]\\&+\frac{m_e}{e^2n_e}\left[\frac{\partial\boldsymbol{J}}{\partial t}+\nabla\boldsymbol{\cdot}\left(\boldsymbol{V}_i\boldsymbol{J}+\boldsymbol{J}\boldsymbol{V}_i-\frac{\boldsymbol{J}\boldsymbol{J}}{en_e}\right)\right],\end{aligned} \tag{1.7}$$

where Faraday's law can be used to write $\partial\boldsymbol{J}/\partial t=-\mu_0^{-1}\nabla\times\nabla\times\boldsymbol{E}$. At this point, upon following a standard procedure in plasma theory, Cheng & Johnson (1999) neglected all terms of the order of m_e/m_i, thereby leading to

$$\begin{aligned}\boldsymbol{E}\;=\;&-\boldsymbol{V}_i\times\boldsymbol{B}+\frac{1}{en_e}\left[\boldsymbol{J}\times\boldsymbol{B}-\nabla\boldsymbol{\cdot}\left(\widetilde{\mathbb{P}}_e-\frac{Zm_e}{m_i}\widetilde{\mathbb{P}}_i\right)\right]\\&+\frac{m_e}{e^2n_e}\left[\frac{\partial\boldsymbol{J}}{\partial t}+\nabla\boldsymbol{\cdot}\left(\boldsymbol{V}_i\boldsymbol{J}+\boldsymbol{J}\boldsymbol{V}_i-\frac{\boldsymbol{J}\boldsymbol{J}}{en_e}\right)\right],\end{aligned} \tag{1.8}$$

https://doi.org/10.1017/S0022377817000381 Published online by Cambridge University Press

where we have recalled that $\widetilde{\mathbb{P}}_i$ is proportional to the ion mass in order to retain ion pressure effects. Also, the relation $m_e/e^2n_e = \mu_0\delta_e^2$ can be used to rewrite the second line of the equation above in terms of the plasma skin depth.

In the present work, we are interested in how electron pressure anisotropy effects manifest in different models. Thus, we shall study the consequences of using the reduced forms (1.6) and (1.8) of Ohm's law in the particular case of the Weibel instability (Weibel 1959). More particularly, we shall consider the implications of both truncated moment models and fully kinetic theories. Also, special emphasis will be given to the comparison between certain kinetic models and their variational versions, which arise from Hamilton's variational principle (Tronci 2013). As we shall see, the approaches based on the simplified Ohm's law (1.6) appear unable to capture pressure anisotropy effects without exhibiting physical inconsistencies. While the first part of the paper focuses on moment truncations, the second part is devoted to fully kinetic theories. Finally, the third part shows how quasi-neutral kinetic models based on the generalized Ohm's laws (1.7) and (1.8) appear to recover all the relevant physical features of the Weibel instability.

2. Moment models

In order to formulate a simplified model for collisionless reconnection, Hesse & Winske (1993) formulated a hybrid model in which ion kinetics is coupled to a moment truncation of the electron kinetic equation, while the electron momentum equation is replaced by Ohm's law (1.6). The problem of moment truncations is still an active area of research (Wang *et al.* 2015) dating back to Grad's work (Grad 1949). In this section, we linearize the Hesse–Winske model to study its dispersion relation in the case of the Weibel instability.

2.1. *The Hesse–Winske moment model*

As anticipated above, the Hesse–Winske (HW) model involves a moment truncation of the electron kinetics. More specifically, the electron kinetic equation is truncated to the second-order moment thereby leading to the following equation for the electron pressure (e.g. see equation (2) in Kuznetsova *et al.* (1998)):

$$\frac{\partial\widetilde{\mathbb{P}}_e}{\partial t} + (\boldsymbol{V}_e\boldsymbol{\cdot}\nabla)\widetilde{\mathbb{P}}_e + (\nabla\boldsymbol{\cdot}\boldsymbol{V}_e)\widetilde{\mathbb{P}}_e + \widetilde{\mathbb{P}}_e\boldsymbol{\cdot}\nabla\boldsymbol{V}_e + (\widetilde{\mathbb{P}}_e\boldsymbol{\cdot}\nabla\boldsymbol{V}_e)^{\mathrm{T}} = \frac{e}{m_e}(\boldsymbol{B}\times\widetilde{\mathbb{P}}_e - \widetilde{\mathbb{P}}_e\times\boldsymbol{B}). \tag{2.1}$$

This equation neglects heat flux contributions and this approximation may or may not be physically consistent depending on the case under study. In a series of papers (Hesse & Winske 1993, 1994; Winske & Hesse 1994; Kuznetsova *et al.* 1998, 2000; Yin *et al.* 2001; Yin & Winske 2003; Hesse *et al.* 2004), the authors approximated heat flux contributions by an isotropization term involving *ad hoc* parameters. However, in this section we shall continue to discard the heat flux, whose corresponding effects will be completely included in our later discussion of fully kinetic models. We address the reader to Basu's work (Basu 2002) and the more recent results in Sarrat, Del Sarto & Ghizzo (2016), Ghizzo, Sarrat & Del Sarto (2017) for a complete description of the Weibel instability in terms of kinetic moments. In addition, we point out that the gyration terms on the right-hand side of (2.1) are discarded in Yin *et al.* (2001), Yin & Winske (2003) (strong electron magnetization assumption), while these terms are retained in the present treatment.

The electron pressure dynamics (2.1) is coupled in the HW model to Faraday's law $\partial \boldsymbol{B}/\partial t = -\nabla \times \boldsymbol{E}$ and the ion kinetics

$$\frac{\partial f_i}{\partial t} + \boldsymbol{v}\cdot\frac{\partial f_i}{\partial \boldsymbol{x}} + \frac{Ze}{m_i}(\boldsymbol{E}+\boldsymbol{v}\times\boldsymbol{B})\cdot\frac{\partial f_i}{\partial \boldsymbol{v}} = 0, \tag{2.2}$$

where the electric field is given by Ohm's law in the form (1.6). In addition, quasi-neutrality gives

$$Zen_i - en_e = 0, \quad Zen_i\boldsymbol{V}_i - en_e\boldsymbol{V}_e = \mu_0^{-1}\nabla\times\boldsymbol{B} = \boldsymbol{J}, \tag{2.3a,b}$$

so that $(n_e, \boldsymbol{V}_e)$ can be expressed in terms of the ion moments.

Since we are interested in the Weibel instability, we linearize the HW model around a static anisotropic equilibrium of the type

$$\boldsymbol{E}_0 = \boldsymbol{B}_0 = \boldsymbol{V}_{e0} = \boldsymbol{V}_{i0} = 0, \quad \mathbb{P}_0 = p_\perp\mathbf{1} + (p_\parallel - p_\perp)\boldsymbol{zz}, \quad f_0 = f_0(v_\perp^2, v_z^2), \tag{2.4a–c}$$

and we consider longitudinal propagation along the wavevector $\boldsymbol{k} = k\boldsymbol{z}$ (here, $\boldsymbol{z}$ denotes the unit vertical). Notice that we have dropped the species subscripts for convenience and we have retained both electron and ion anisotropies. The corresponding dispersion relation is found in § A.1 and it reads

$$\frac{\omega^2}{k^2 v_{e\parallel}^2} = 1 - \frac{T_\perp^{(e)}}{T_\parallel^{(e)}} + k^2\delta_e^2 + Z\bar{\mu}\left[1 + \frac{T_\perp^{(i)}}{T_\parallel^{(i)}} W\left(\frac{\omega}{kv_{i\parallel}}\right)\right], \tag{2.5}$$

where $\bar{\mu} = m_e/m_i$.

In order to distinguish the various contributions from the ions and the electrons, it is useful to study the electron Weibel instability and the ion Weibel instability separately. In the first case, one can restrict to an isotropic ion equilibrium, so that $T_\perp^{(i)} = T_\parallel^{(i)}$. In addition, upon adopting a cold-fluid closure for the ion dynamics one can write $W(\omega/kv_{i\parallel}) \simeq 0$ to obtain

$$\frac{\omega^2}{k^2 v_\parallel^2} = 1 - \frac{T_\perp^{(e)}}{T_\parallel^{(e)}} + k^2\delta^2 + Z\bar{\mu}. \tag{2.6}$$

A detailed discussion of the dispersion relation (2.6) is presented later in the paper. For the moment, we remark that ω is imaginary only in the range $k^2\delta^2 < T_\perp^{(e)}/T_\parallel^{(e)} - Z\bar{\mu} - 1$, while purely oscillating modes emerge otherwise.

The ion Weibel instability can be studied in a similar way upon setting $T_\perp^{(e)} = T_\parallel^{(e)}$ in (2.5) so that, upon restoring the species index and by denoting by v_e the electron thermal velocity, we have

$$\frac{\omega^2}{k^2 v_e^2} - k^2\delta_e^2 = Z\bar{\mu}\left[1 + \frac{T_\perp^{(i)}}{T_\parallel^{(i)}} W\left(\frac{\omega}{kv_{i\parallel}}\right)\right]. \tag{2.7}$$

Again, this dispersion relation is discussed later in this paper.

2.2. *The effect of Coriolis force terms*

In Tronci (2013), one of us showed how one can neglect the electron mean-flow inertia terms in (1.5) by using variational methods based on Hamilton's principle. This approach has the advantage of preserving the total energy and momentum and in recent years there is an increasing amount of work in exploiting this approach for nonlinear plasma modelling (Cendra *et al.* 1998; Morrison 1998; Brizard 2000; Holm & Tronci 2012; Tronci & Camporeale 2015). Essentially, in plasma physics this approach goes back to Low (1958), Newcomb (1962) and it was later used in Littlejohn (1983) in his theory of guiding-centre motion. When applied to the case under study, this method produces Coriolis forces in the electron kinetics that modify the electron pressure dynamics (2.1) in the HW model as follows:

$$\frac{\partial\widetilde{\mathbb{P}}_e}{\partial t}+(\boldsymbol{V}_e\boldsymbol{\cdot}\nabla)\widetilde{\mathbb{P}}_e+(\nabla\boldsymbol{\cdot}\boldsymbol{V}_e)\widetilde{\mathbb{P}}_e+\widetilde{\mathbb{P}}_e\boldsymbol{\cdot}\nabla\boldsymbol{V}_e+(\widetilde{\mathbb{P}}_e\boldsymbol{\cdot}\nabla\boldsymbol{V}_e)^{\mathrm{T}} \\ +\widetilde{\mathbb{P}}_e\times\left(\frac{e}{m_e}\boldsymbol{B}+\boldsymbol{\omega}_e\right)-\left(\frac{e}{m_e}\boldsymbol{B}+\boldsymbol{\omega}_e\right)\times\widetilde{\mathbb{P}}_e=0, \tag{2.8}$$

where $\boldsymbol{\omega}_e=\nabla\times\boldsymbol{V}_e$ denotes the electron hydrodynamic vorticity. As shown in Tronci (2013), the vorticity terms arise by neglecting the electron mean-flow inertia after expressing the electron kinetics in the relative frame moving with the Eulerian velocity $\boldsymbol{V}_e$; this takes the dynamics in a non-inertial frame thereby producing Coriolis forces that shift the magnetic field by the electron vorticity. We remark that the terms involving the electron velocity (including the vorticity terms) combine into a fluid transport operator (Lie derivative) so that the electron pressure becomes frozen into the electron mean flow in the case of strong electron magnetization (so that $(\boldsymbol{e}/\boldsymbol{m}_e)\widetilde{\mathbb{P}}_e\times\boldsymbol{B}-(\boldsymbol{e}/\boldsymbol{m}_e)\boldsymbol{B}\times\widetilde{\mathbb{P}}_e\simeq 0$). At this point, the Coriolis forces in the electron pressure dynamics lead to a modified version of the HW model.

Upon linearizing the modified HW model around the equilibrium (2.4*a-c*), one obtains the dispersion relation (see § A.1)

$$\frac{\omega^2}{k^2v_{e\parallel}^2}=1-\frac{T_\perp^{(e)}}{T_\parallel^{(e)}}\left\{1-k^2\delta_e^2-\frac{Zm_e}{m_i}\left[1+\frac{T_\perp^{(i)}}{T_\parallel^{(i)}}W\left(\frac{\omega}{kv_{i\parallel}}\right)\right]\right\}. \tag{2.9}$$

By proceeding analogously to the previous section, we consider the electron Weibel instability by setting $T_\perp^{(i)}=T_\parallel^{(i)}$ and $W(\omega/kv_{i\parallel})\simeq 0$ thereby obtaining

$$\frac{\omega^2}{k^2v_\parallel^2}=1-\frac{T_\perp^{(e)}}{T_\parallel^{(e)}}+\frac{T_\perp^{(e)}}{T_\parallel^{(e)}}\left(k^2\delta^2+Z\bar{\mu}\right). \tag{2.10}$$

Again, we notice that ω is imaginary only in the range $k^2\delta^2<1-Z\bar{\mu}-T_\parallel^{(e)}/T_\perp^{(e)}$, while purely oscillating modes emerge otherwise.

In the same way, we can specialize (2.9) to the case of the ion Weibel instability. In this case, Coriolis effects become irrelevant and one obtains again equation (2.7).

The next section presents a study of (2.5) and (2.9) in each considered case.

2.3. *Discussion on moment models*

Here and in the following discussions, we consider an electron–proton plasma, with typical solar wind parameters. For comparison, we report the following dispersion

https://doi.org/10.1017/S0022377817000381 Published online by Cambridge University Press

relation corresponding to full Vlasov–Maxwell dynamics (see e.g. Gary & Karimabadi (2006)), as it is obtained by using the exact form of Ohm's law (1.7):

$$1+\frac{T_\perp^{(e)}}{T_\parallel^{(e)}}W\left(\frac{\omega}{kv_{e\parallel}}\right)=\frac{\omega^2}{\omega_{pe}^2}-k^2\delta_e^2-Z\bar{\mu}\frac{T_\perp^{(i)}}{T_\parallel^{(i)}}\left[1+W\left(\frac{\omega}{kv_{i\parallel}}\right)\right]. \tag{2.11}$$

Here, the electron Weibel instability is studied by adopting a cold-fluid closure for ion kinetics, so that $T_\perp^{(i)}=T_\parallel^{(i)}$ and $W(\omega/kv_{i\parallel})\simeq 0$ yield

$$1+\frac{T_\perp^{(e)}}{T_\parallel^{(e)}}W\left(\frac{\omega}{kv_{e\parallel}}\right)=\frac{\omega^2}{\omega_{pe}^2}-k^2\delta_e^2-Z\bar{\mu}. \tag{2.12}$$

The ratio between electron thermal velocity (in the cold direction) and speed of light $v_e/c=0.0318$ (this is also the ratio between Debye length and electron inertial length). The mass ratio is physical $m_i/m_e=1836$. Figures 1 and 2 show the dispersion relations for electron and ion Weibel instabilities, respectively. The four panels are for values of temperature anisotropy equal to 2, 5, 10 and 100. The blue lines show the reference solutions derived from the Vlasov–Maxwell model (2.12) (involving a cold-fluid closure for ion kinetics), while red lines are for (2.6). In figure 1 one can notice how the HW model yields much larger growth rates than the correct values. The results for the modified HW model (2.10) are shown in yellow. They partially correct the discrepancies with the full Vlasov–Maxwell model, but they are still unsatisfactory, especially for wavevectors larger than the inverse electron inertial length.

As we mentioned, the Coriolis effects are irrelevant for the case of the ion Weibel instability. In this case, the reference Vlasov solution is obtained in figure 2 by solving the dispersion relation

$$1+\frac{k^2v_{e\parallel}^2}{2\omega^2}=\frac{\omega^2}{\omega_{pe}^2}-k^2\delta_e^2-Z\bar{\mu}\frac{T_\perp^{(i)}}{T_\parallel^{(i)}}\left[1+W\left(\frac{\omega}{kv_{i\parallel}}\right)\right]. \tag{2.13}$$

This is derived upon adopting a warm-fluid closure for electron kinetics, that is by inserting $T_\perp^{(e)}=T_\parallel^{(e)}$ and $W(\omega/kv_{e\parallel})\simeq(1/2)k^2v_{e\parallel}^2/\omega^2$ in (2.11). Interestingly, for the ion Weibel instability the discrepancies between the HW and VM models are already significant for $k\delta_e<0.1$.

3. Electron inertia in fully kinetic theories

While the results in the previous sections were obtained by using moment truncations, one is led to ask about the effects arising from higher moments. In order to address this point, this section presents two different ways to neglect the electron mean-flow inertia in a fully kinetic theory, in such a way that all higher moments are fully considered. We remark that this is an unprecedented approach in the plasma physics literature, with the exception of Tronci (2013). By following the discussion therein, we remark that it may not be convenient to implement this approximation directly in the electron kinetic equation

$$\frac{\partial f_e}{\partial t}+\boldsymbol{v}\cdot\frac{\partial f_e}{\partial \boldsymbol{x}}-\frac{e}{m_e}(\boldsymbol{E}+\boldsymbol{v}\times\boldsymbol{B})\cdot\frac{\partial f_e}{\partial \boldsymbol{v}}=0. \tag{3.1}$$

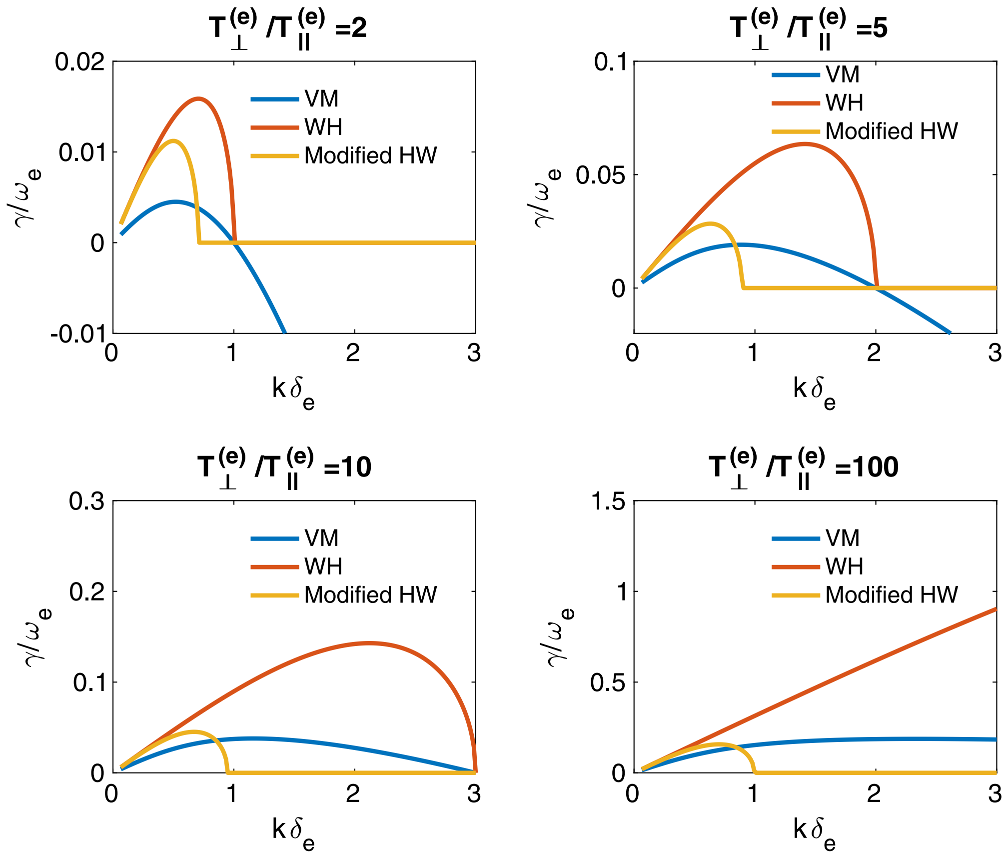

FIGURE 1. Growth rate for the electron Weibel instability for the HW (2.6) and modified HW (2.10) models, for four values of temperature anisotropy $T_\perp^{(e)}/T_\parallel^{(e)}=2, 5, 10, 100$. The blue lines are the reference solutions derived from the Vlasov–Maxwell model, while red and yellow lines are for (2.6) and (2.10), respectively.

Indeed, doing this would generate questions of compatibility between the above electron kinetics and the reduced form of Ohm's law (1.6), which we want to adopt throughout this section as a first step in neglecting the electron mean-flow inertia. Before making any assumption, it is instead convenient to express electron kinetics in the mean-flow frame by introducing the coordinate $\boldsymbol{c}=\boldsymbol{v}-\boldsymbol{V}_e$ and looking at the dynamics for the relative distribution

$$\mathrm{f}_e(\boldsymbol{x}, \boldsymbol{c}, t) = f_e(\boldsymbol{x}, \boldsymbol{c}+\boldsymbol{V}_e, t), \tag{3.2}$$

that is

$$\frac{\partial \mathrm{f}_e}{\partial t} + (\boldsymbol{c}+\boldsymbol{V}_e)\boldsymbol{\cdot}\frac{\partial \mathrm{f}_e}{\partial \boldsymbol{x}} - \left\{\frac{\mathrm{D}\boldsymbol{V}_e}{\mathrm{D}t} + (\boldsymbol{c}\boldsymbol{\cdot}\nabla)\boldsymbol{V}_e + \frac{e}{m_e}[\boldsymbol{E}+(\boldsymbol{c}+\boldsymbol{V}_e)\times\boldsymbol{B}]\right\}\boldsymbol{\cdot}\frac{\partial \mathrm{f}_e}{\partial \boldsymbol{c}} = 0. \tag{3.3}$$

In turn, this kinetic equation is accompanied by Ampère's law and Faraday's law. At this stage, one still needs a closure for the electric field, which can be obtained by writing Ohm's law. The latter arises from taking the first moment of (3.3) and

https://doi.org/10.1017/S0022377817000381 Published online by Cambridge University Press

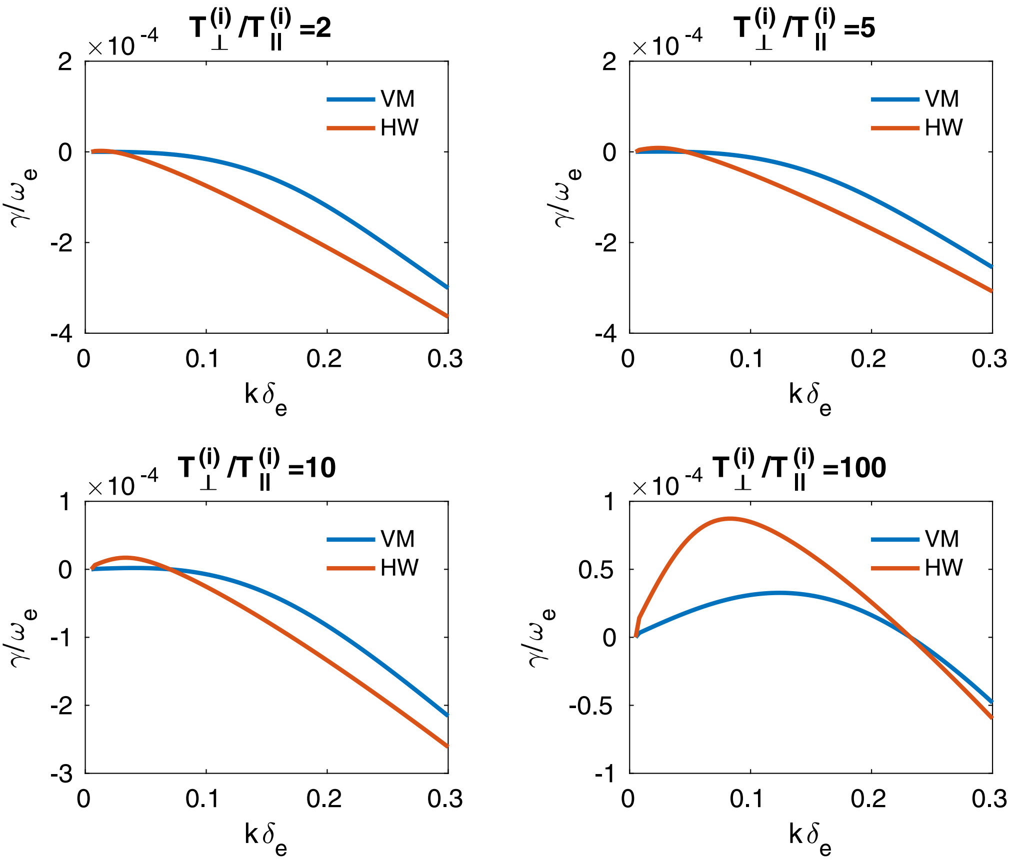

FIGURE 2. Growth rate for the ion Weibel instability for the HW (2.5) model, for four values of temperature anisotropy $T_{\perp}^{(i)}/T_{\parallel}^{(i)} = 2, 5, 10, 100$. The blue lines are the reference solutions derived from the Vlasov–Maxwell model, while red lines are for (2.5). In this case the modified HW model (2.9) yields identical results.

by using the constraint $\int \boldsymbol{c}\, \mathsf{f}_e(\boldsymbol{c})\, \mathrm{d}\boldsymbol{c} = 0$; this process leads to equation (1.1). So far, no approximation was performed and the mean-flow electron inertia is still fully retained, as it is made explicit by multiplying (3.3) by $m_e n_e$. Indeed, we notice that the first term in the acceleration field multiplying $\partial \mathsf{f}_e/\partial \boldsymbol{c}$ in (3.3) is precisely the term neglected in Ohm's law (1.5) to obtain its reduced form (1.6). This acceleration term can also be expanded as

$$\frac{\mathrm{D}\boldsymbol{V}_e}{\mathrm{D}t} = \frac{\partial \boldsymbol{V}_e}{\partial t} - \boldsymbol{V}_e \times (\boldsymbol{\nabla} \times \boldsymbol{V}_e) + \frac{1}{2}\boldsymbol{\nabla}|\boldsymbol{V}_e|^2, \tag{3.4}$$

which evidently corresponds to a superposition of inertial forces excerpted by the mean flow on the particles moving in the relative frame.

In the next section, we shall present two different possible strategies for implementing the assumption of negligible electron mean-flow inertia. While the first approach is direct and involves the equations of motion, the second approach is based on variational methods and it involves Hamilton's principle. Although the second approach removes some of the inconsistencies emerging from the first, both methods appear to be unsatisfactory for a complete description of the Weibel instability.

https://doi.org/10.1017/S0022377817000381 Published online by Cambridge University Press

3.1. *Removing the electron inertia*

A first approach to neglect electron inertia consists of simply removing the term $-\mathrm{D}\boldsymbol{V}_e/\mathrm{D}t$ in (3.3), thereby leading to the modified electron equation

$$\frac{\partial \mathsf{f}_e}{\partial t}+(\boldsymbol{c}+\boldsymbol{V}_e)\boldsymbol{\cdot}\frac{\partial \mathsf{f}_e}{\partial \boldsymbol{x}}-\left\{\boldsymbol{c}\boldsymbol{\cdot}\nabla\boldsymbol{V}_e+\frac{e}{m_e}[\boldsymbol{E}+(\boldsymbol{c}+\boldsymbol{V}_e)\times\boldsymbol{B}]\right\}\boldsymbol{\cdot}\frac{\partial \mathsf{f}_e}{\partial \boldsymbol{c}}=0. \tag{3.5}$$

Although this equation retains the acceleration term $-\boldsymbol{c}\boldsymbol{\cdot}\nabla\boldsymbol{V}_e$, inertial forces are only partially considered since the term (3.4) has been entirely neglected. At this point, one can easily take the first moment of (3.5), so that using the constraint $\int \boldsymbol{c}\,\mathsf{f}_e(\boldsymbol{c})\,\mathrm{d}\boldsymbol{c}=0$ leads to the reduced Ohm's law (1.6) and a fully kinetic model is formulated by using ion kinetics (2.2), along with Ampère's and Faraday's laws.

The model obtained in this way provides the basis for the HW moment model in § 2.1, except that the HW model invokes the quasi-neutrality conditions (2.3). The idea of using quasi-neutrality in a fully kinetic model is not new. In later sections, we shall show how the quasi-neutrality assumption can be used successfully in fully kinetic theories, although it requires extra care. However, for the purpose of this section, we shall keep assuming quasi-neutrality in the present discussion. Thus, Ampère's law in (2.3) can be used to eliminate entirely the variable $\boldsymbol{V}_e$ in favour of the ion velocity $\boldsymbol{V}_i$, as it is computed from (2.2).

Combining (2.2), (3.5), (2.3) and Faraday's law yields a fully kinetic model, whose moment truncation to second-order yields exactly the HW moment model from § 2.1. For later reference, we shall refer to this as the *HW kinetic model*. Then, one would hope that completing the HW moment model by retaining fully kinetic effects (while still neglecting electron mean-flow inertia) could capture more physics. As we shall see, this may not always be true and we explain this below by considering again the case of the Weibel instability.

Here, we linearize the HW kinetic model around the bi-Maxwellian equilibrium

$$\boldsymbol{E}_0=\boldsymbol{B}_0=0,\quad f_0=f_0(v_\perp^2,\,v_z^2),\quad \mathsf{f}_0=\mathsf{f}_0(c_\perp^2,\,c_z^2), \tag{3.6}$$

where f_0 and f_0 denote the ionic and electronic equilibrium, respectively. As shown in § A.2, we obtain the dispersion relation

$$1+\frac{T_\perp^{(e)}}{T_\parallel^{(e)}}W\left(\frac{\omega}{kv_{e\parallel}}\right)=\left\{k^2\delta_e^2+Z\bar{\mu}\left[1+\frac{T_\perp^{(i)}}{T_\parallel^{(i)}}W\left(\frac{\omega}{kv_{i\parallel}}\right)\right]\right\}W\left(\frac{\omega}{kv_{e\parallel}}\right). \tag{3.7}$$

In order to study the electron Weibel instability, we follow the approach in § 2.1 and adopt a cold-fluid closure for the ions by setting $T_\perp^{(i)}=T_\parallel^{(i)}$ and $W(\omega/kv_{i\parallel})\simeq 0$. This yields

$$1+\frac{T_\perp^{(e)}}{T_\parallel^{(e)}}W\left(\frac{\omega}{kv_{e\parallel}}\right)=(k^2\delta_e^2+Z\bar{\mu})\,W\left(\frac{\omega}{kv_{e\parallel}}\right). \tag{3.8}$$

On the other hand, the ion Weibel instability requires special care since Ohm's law (1.6) requires pressure to balance the Lorentz force in electron dynamics. Indeed, as one can see especially in (A 14) in § A.1, adopting a cold-fluid closure for electron dynamics would lead to consistency issues. However, a warm-fluid closure can be performed by setting $T_\perp^{(e)}=T_\parallel^{(e)}$ and $W(\omega/kv_{e\parallel})\simeq(1/2)k^2v_{e\parallel}^2/\omega^2$ so that (3.7) becomes

$$\frac{2\omega^2}{k^2v_{e\parallel}^2}-k^2\delta_e^2=Z\bar{\mu}\left[1+\frac{T_\perp^{(i)}}{T_\parallel^{(i)}}W\left(\frac{\omega}{kv_{i\parallel}}\right)\right]-1. \tag{3.9}$$

https://doi.org/10.1017/S0022377817000381 Published online by Cambridge University Press

The contribution of the heat flux and higher moments can be understood by comparing the above equation to the corresponding equation (2.7) for the HW moment model.

While the discussion of the dispersion relations (3.8) and (3.9) is left for later discussion, the next section aims at extending the modified HW moment model from § 2.2 to a fully kinetic theory.

3.2. *Coriolis force effects*

A modified version of the HW kinetic model was presented in Tronci (2013) (see equations (1)–(5) therein), by exploiting variational techniques based on Hamilton's principle. As discussed in § 2.2, this approach produces the Coriolis force terms appearing in (2.8). In the fully kinetic treatment, the same approach leaves (2.2), (2.3) and Faraday's law unchanged while (3.5) is modified as follows:

$$\frac{\partial \mathsf{f}_e}{\partial t}+(\boldsymbol{c}+\boldsymbol{V}_e)\cdot\frac{\partial \mathsf{f}_e}{\partial \boldsymbol{x}}-\left\{\boldsymbol{c}\cdot\nabla\boldsymbol{V}_e+\boldsymbol{c}\times\nabla\times\boldsymbol{V}_e+\frac{e}{m_e}[\boldsymbol{E}+(\boldsymbol{c}+\boldsymbol{V}_e)\times\boldsymbol{B}]\right\}\cdot\frac{\partial \mathsf{f}_e}{\partial \boldsymbol{c}}=0. \tag{3.10}$$

Evidently, this differs from (3.5) by the Coriolis acceleration term $\boldsymbol{c}\times\nabla\times\boldsymbol{V}_e$. As discussed in Tronci (2013), this term appears from the variational approach due to the fact that the change of frame performed to express the electron kinetics in the mean-flow frame affects the Lorentz force term, which now is written in terms of the effective magnetic field $\boldsymbol{B}+m_e\boldsymbol{\omega}_e/e$. This is a typical feature of electrodynamics in non-inertial frames, as explained in Thyagaraja & McClements (2009). Notice that the Coriolis acceleration term is absent in (3.3), which also means that this term is produced to guarantee a consistent force balance after the mean-flow inertia term $\mathrm{D}\boldsymbol{V}_e/\mathrm{D}t$ is dropped in (3.3). At this point, the modified HW kinetic model is given by (3.10), (2.2), (2.3) and Faraday's law.

For comparison with the HW kinetic model in the previous section, we study the effect of Coriolis forces by considering again the Weibel instability. Then, we linearize the modified HW kinetic system around the equilibrium (3.6) to obtain the dispersion relation (see § A.2)

$$1+\frac{T_\perp^{(e)}}{T_\parallel^{(e)}}W\left(\frac{\omega}{kv_{e\parallel}}\right)=\frac{T_\perp^{(e)}}{T_\parallel^{(e)}}\left\{k^2\delta_e^2+Z\bar{\mu}\left[1+\frac{T_\perp^{(i)}}{T_\parallel^{(i)}}W\left(\frac{\omega}{kv_{i\parallel}}\right)\right]\right\}W\left(\frac{\omega}{kv_{e\parallel}}\right). \tag{3.11}$$

By following the approach in the previous sections, we restrict to consider the electron Weibel instability by adopting a cold-fluid closure for the ions. This yields

$$\frac{T_\parallel^{(e)}}{T_\perp^{(e)}}+W\left(\frac{\omega}{kv_{e\parallel}}\right)=(k^2\delta_e^2+Z\bar{\mu})\,W\left(\frac{\omega}{kv_{e\parallel}}\right). \tag{3.12}$$

On the other hand, upon assuming a warm-fluid closure for the electrons by replacing $T_\perp^{(e)}=T_\parallel^{(e)}$ and $W(\omega/kv_{e\parallel})\simeq(1/2)k^2v_{e\parallel}^2/\omega^2$ in (3.11), we obtain the same dispersion relation (3.9) for the ion Weibel instability.

3.3. *Discussion on kinetic models with inertialess electrons*

In first instance, this section compares the dispersion relations (3.8) and (3.11) for the electron Weibel instability with the corresponding result (2.12) for the case of the

https://doi.org/10.1017/S0022377817000381 Published online by Cambridge University Press

Vlasov–Maxwell system for cold-fluid ions. A typical limit that is often used to study the Weibel instability is

$$\omega \ll k v_{e\parallel} \tag{3.13}$$

so that $W(\omega/kv_{e\parallel}) \simeq -1 - i\sqrt{\pi}\,\omega/kv_{e\parallel}$. In this limit, equations (3.8) and (3.11) become (upon dropping the species superscript for convenience)

$$-\mathrm{i}\omega = \frac{kv_{\parallel}}{\sqrt{\pi}}\left(1 + \frac{1}{T_{\perp}/T_{\parallel} - k^2\delta^2 - Z\bar{\mu}}\right) \tag{3.14}$$

and

$$-\mathrm{i}\omega = \frac{kv_{\parallel}}{\sqrt{\pi}}\left(1 - \frac{T_{\parallel}}{T_{\perp}}\frac{1}{1 - k^2\delta^2 - Z\bar{\mu}}\right), \tag{3.15}$$

respectively. On the other hand, upon assuming $\omega \ll \omega_p$, equation (2.12) becomes

$$-\mathrm{i}\omega = \frac{kv_{\parallel}}{\sqrt{\pi}}\left[1 - \frac{T_{\parallel}}{T_{\perp}}(k^2\delta^2 + Z\bar{\mu} + 1)\right]. \tag{3.16}$$

Now, we observe that in the limit $k\delta \ll 1$ the results in (3.15) and (3.16) coincide thereby showing that the variational model from § 2.2 agrees well with Vlasov–Maxwell dynamics for length scales much bigger than the skin depth. In turn, in the same limit $k\delta \ll 1$ (3.14) disagrees with the Vlasov–Maxwell result (3.16) with growing anisotropies.

However, both results (3.14) and (3.15) suffer from the important drawback that a vertical asymptote emerges in the growth rate as length scales approach the skin depth. We remark that the assumption $\omega \ll kv_{e\parallel}$ is no longer valid near and after the asymptote and so the dispersion relation needs to be solved numerically, as presented below. After the asymptotes, for both kinetic models the least damped mode is not the Weibel mode, but one with non-zero real frequency, hence yielding a completely different result from the Vlasov–Maxwell theory, in which the Weibel (purely damping) mode is dominant. Figure 3 shows the dispersion relations for the electron instability, for four values of temperature anisotropy $T_{\perp}^{(e)}/T_{\parallel}^{(e)} = 2, 5, 10, 100$. The blue lines are the reference solutions derived from the Vlasov–Maxwell model (2.12), while red and yellow lines are for the HW kinetic (3.8) and modified HW kinetic (3.12) models, respectively. The aforementioned asymptote for the reduced models is clearly visible, with the distinguishing features that while it always occurs at $k\delta = 1$ for the modified HW model, it becomes a function of anisotropy for the HW model. Both models present large discrepancies with respect to the full Vlasov–Maxwell solution, with the wavevector approaching the inverse electron inertial length. Figure 4 shows the real frequency of the least damped mode for the modified HW kinetic model (solid lines) and for the HW kinetic model (dashed lines). Once again, in contrast with the correct VM solution, the mode's real frequency becomes non-zero after the respective asymptote.

The ion Weibel instability is, on the contrary, well captured by both models. This is shown in figure 5. Once again, in this case the Coriolis correction does not play any role and the two models become identical. One can notice that, for any value of temperature anisotropy, the solutions are indistinguishable from the correct Vlasov–Maxwell results, which are obtained from the dispersion relation (2.13) (adopting a warm-fluid closure for the electrons). In some sense, this is not surprising, since ion kinetics is not subject to any approximation in either the HW kinetic model and its modified variant.

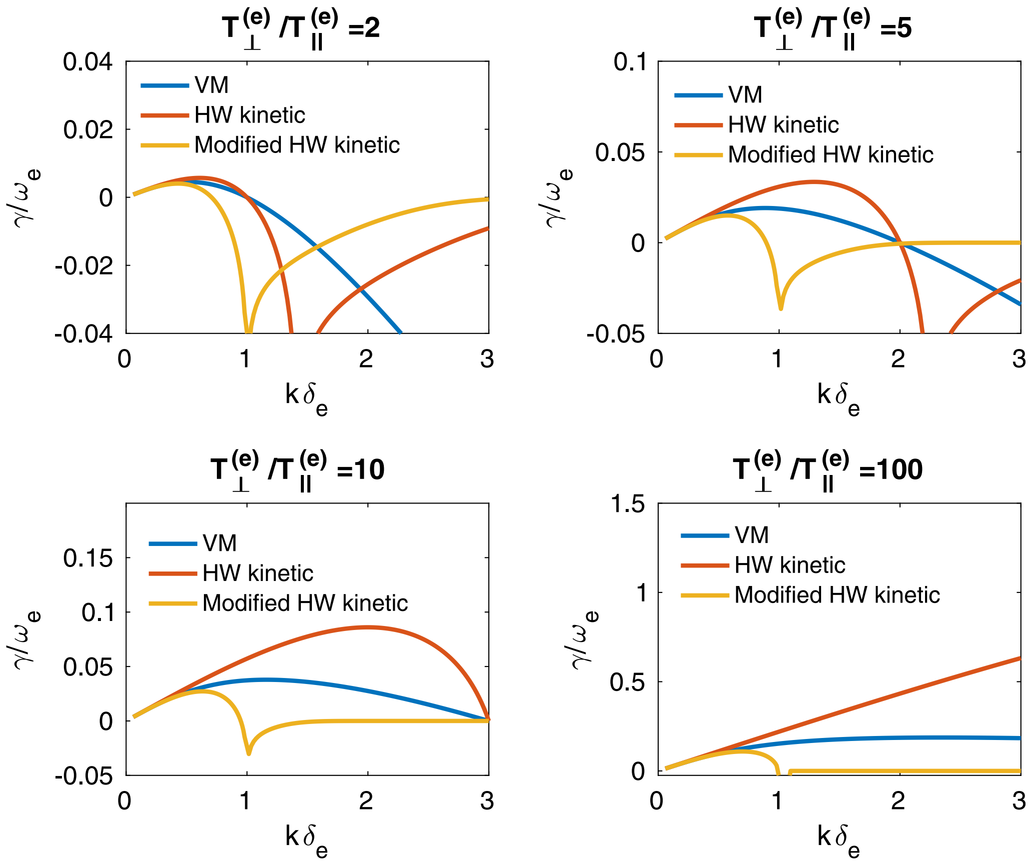

FIGURE 3. Growth rate for the electron Weibel instability for the HW kinetic (3.8) and modified HW kinetic (3.12) models, for four values of temperature anisotropy $T_\perp^{(e)}/T_\parallel^{(e)} = 2, 5, 10, 100$. The blue lines are the reference solutions derived from the Vlasov–Maxwell model, while red and yellow lines are for (3.8) and (3.12), respectively.

4. Quasi-neutral Vlasov theories

We have shown that all the moment models and fully kinetic theories considered so far and aiming at neglecting the electron inertia in Ohm's law (1.5) suffer from different drawbacks. More specifically, in the nonlinear regime unphysical modes with $k\delta > 1$ may be excited even if $k\delta \ll 1$ at the initial time. Even the variational approach in Tronci (2013), while correcting certain discrepancies in the electron Weibel instability and retaining the full physics of the ion Weibel instability, would need an appropriate numerical filtering to prevent the dynamics from introducing length scales of the order of (or smaller than) the electron skin depth. On the other hand, the analysis performed so far also posed an alternative question about the validity of the quasi-neutral limit in fully kinetic theories. Indeed, the assumption of quasi-neutrality (2.3) was used throughout all the discussion thereby leading to the question of whether quasi-neutrality may also produce consistency issues when implemented in a fully kinetic theory. A first answer to this question was provided by Cheng and Johnson in Cheng & Johnson (1999), where quasi-neutrality was assumed in the Vlasov–Maxwell system, along with the generalized Ohm's law (1.8). In this

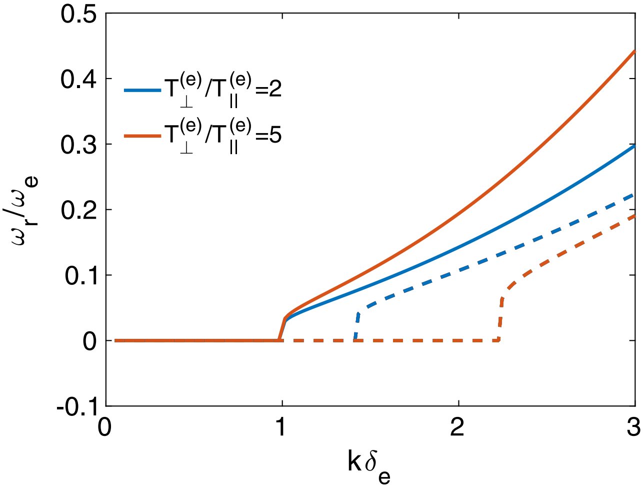

FIGURE 4. Real part of the frequency for the electron Weibel instability for the modified HW kinetic model (3.12) (solid lines) and for the KW kinetic model (3.8) (dashed lines), for values of temperature anisotropy $T_\perp^{(e)}/T_\parallel^{(e)} = 2, 5$.

approach, all terms of the order of m_e/m_i are considered irrelevant and thus are ignored. On the other hand, these terms were considered in more recent work by the authors (Tronci & Camporeale 2015), where quasi-neutrality was invoked at the level of Hamilton's variational principle. The model in Tronci & Camporeale (2015) was dubbed the *neutral Vlasov model*.

In the following sections, we present both the Cheng–Johnson (CJ) model (Cheng & Johnson 1999) and the neutral Vlasov model (Tronci & Camporeale 2015). As we shall see, both models reproduce faithfully the physics of both ion and electron Weibel instabilities. In addition, we shall see how Ampère's current balance may play a crucial role in preserving quasi-neutrality at all times; this point is of particular interest for the CJ model, where the exact current balance is lost, while it is retained by the *neutral Vlasov model*.

4.1. *The Cheng–Johnson model*

As anticipated above, Cheng & Johnson (1999) were the first to design an alternative fully kinetic model in the quasi-neutral limit. More specifically, they expanded Ohm's law (1.1) by using Ampeère's and Faraday's laws to obtain (1.7). Then, after assuming quasi-neutrality to write $\boldsymbol{J} = \mu_0^{-1}\boldsymbol{\nabla} \times \boldsymbol{B}$, they neglected all terms of the order of m_e/m_i. This process leads to the reduced form of Ohm's law in (1.8), which is then accompanied by the kinetic equations (2.2) and (3.1), the quasi-neutrality conditions (2.3) and Faraday's law. We remark that originally the CJ model was called a *kinetic-multifluid system* because the kinetic equation for each species was written to accompany the equation for its first moment. However, this is totally equivalent to retaining only the kinetic equations.

In order to compare the CJ model to the systems formulated in the previous section, we studied the Weibel instability by linearizing again around the equilibrium (3.6). Upon linearizing the CJ model around the bi-Maxwellian equilibrium

$$\boldsymbol{E}_0 = \boldsymbol{B}_0 = 0, \qquad f_{s0} = f_{s0}(v_\perp^2, v_z^2) \tag{4.1}$$

https://doi.org/10.1017/S0022377817000381 Published online by Cambridge University Press

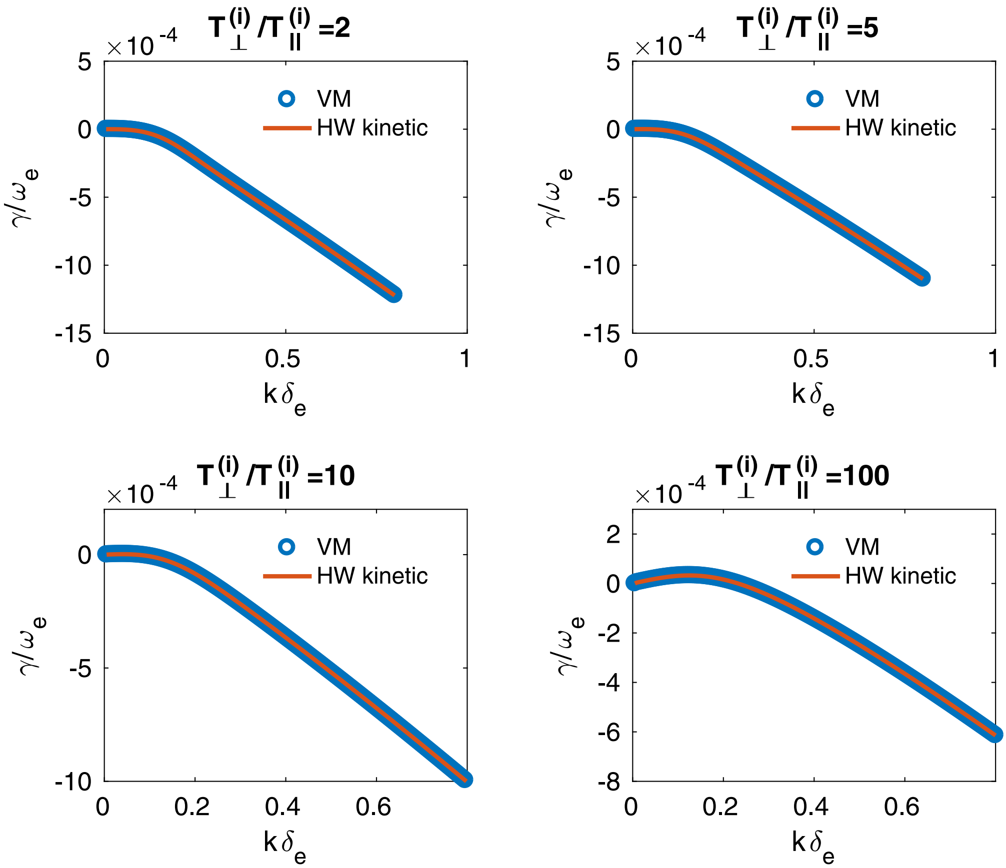

FIGURE 5. Growth rate for the ion Weibel instability for the HW kinetic model (3.7), for four values of temperature anisotropy $T_\perp^{(i)}/T_\parallel^{(i)}=2, 5, 10, 100$. The blue circles denote the reference solutions derived from the Vlasov–Maxwell model, while red lines are for (3.7).

(where the subscript s refers to the particle species), we obtain the dispersion relation (see § A.3)

$$1+\frac{T_\perp^{(e)}}{T_\parallel^{(e)}}W\left(\frac{\omega}{kv_{e\parallel}}\right)=-k^2\delta_e^2-Z\bar{\mu}\frac{T_\perp^{(i)}}{T_\parallel^{(i)}}W\left(\frac{\omega}{kv_{i\parallel}}\right). \tag{4.2}$$

The above dispersion relation can be compared directly with the relation (2.11) that is obtained for the full Vlasov–Maxwell dynamics. As expected, both electron and ion Weibel instabilities are reproduced by the CJ model in exceptional agreement with the full Vlasov–Maxwell theory.

A point about the CJ model that has been omitted so far (while it deserves some attention) is that the quasi-neutrality conditions (2.3) are not preserved in time exactly, as it can be verified by a direct calculation. More specifically, one can ask if the electron velocity as computed from the first moment of (3.1) is compatible with the corresponding expression arising from (2.3). In order to provide the answer to this question, we use (2.3) and the first moment equation of (2.2) to rewrite (1.8) as

$$\boldsymbol{E}=-\boldsymbol{V}_i\times\boldsymbol{B}+\left(1+\frac{Z\bar{\mu}}{1-Z\bar{\mu}}\right)\left(\frac{1}{en_e}\boldsymbol{J}\times\boldsymbol{B}-\frac{1}{en_e}\boldsymbol{\nabla}\boldsymbol{\cdot}\widetilde{\mathbb{P}}_e-\frac{m_e}{e}\frac{\mathrm{D}\boldsymbol{V}_e}{\mathrm{D}t}\right). \tag{4.3}$$

https://doi.org/10.1017/S0022377817000381 Published online by Cambridge University Press

Then, we use (4.3) as the CJ closure equation for the electric field in (3.1). Taking the first moment (here denoted by $\boldsymbol{K}_e$) of the resulting electron kinetic equation yields

$$\begin{aligned}
&\frac{\partial}{\partial t}(\boldsymbol{K}_e - n_e\boldsymbol{V}_e) + \boldsymbol{V}_e \boldsymbol{\cdot} \nabla (\boldsymbol{K}_e - n_e\boldsymbol{V}_e) + \nabla \boldsymbol{\cdot} (\boldsymbol{V}_e\boldsymbol{K}_e - n_e\boldsymbol{V}_e\boldsymbol{V}_e) \\
&\quad = (\boldsymbol{K}_e - n_e\boldsymbol{V}_e) \times \left(\boldsymbol{\omega}_e - \frac{e}{m_e}\boldsymbol{B}\right) + \frac{Z\bar{\mu}}{1-Z\bar{\mu}}\left(\frac{1}{m_e}\boldsymbol{J}\times\boldsymbol{B} - \frac{1}{m_e}\nabla\boldsymbol{\cdot}\widetilde{\mathbb{P}}_e - n_e\frac{\mathrm{D}\boldsymbol{V}_e}{\mathrm{D}t}\right),
\end{aligned} \tag{4.4}$$

where we recall that $\boldsymbol{\omega}_e = \nabla \times \boldsymbol{V}_e$ is the electron vorticity and $(n_e, \boldsymbol{V}_e)$ are expressed by using (2.3). Then, we conclude that the consistency relation $\boldsymbol{K}_e = n_e\boldsymbol{V}_e$ fails to be preserved in time. This is a fundamental consistency issue that is intrinsic to the model and can lead to different drawbacks beyond the linear analysis of the Weibel instability. For example, charge conservation is dramatically affected, thereby preventing neutrality from being satisfied at all times. In the next section, we show how this issue is solved by simply retaining all terms in the exact Ohm's law (1.7).

4.2. *The neutral Vlasov model*

Recently, upon retaining all terms in the exact Ohm's law (1.7), we showed (Tronci & Camporeale 2015) how the quasi-neutral limit can be consistently implemented in the Vlasov–Maxwell system both directly (by formally letting $\epsilon_0 \to 0$) and in Hamilton's variational principle: a comparison with the full Vlasov–Maxwell system was presented and good agreement was found in the linear case for both Alfvèn and Whistler modes at different angles of propagation. Later, Burby (2015) showed how this model also possesses a Hamiltonian structure, while Degond, Deluzet & Doyen (2017) provided an alternative mathematical footing by exploiting scaling and asymptotic techniques in the case of one particle species (by preventing ion motion). In the same work, the question of the numerical implementation was also discussed. As it was presented in Tronci & Camporeale (2015), the quasi-neutral model consists of the kinetic equations (2.2) and (3.1), the quasi-neutrality conditions (2.3), Faraday's law and Ohm's law (1.1). Here, the electron velocity is expressed in terms of the ion velocity by using Ampère's law.

A question that emerged at the end of § 4.1 concerned the possibility of consistency issues precisely with the second equation in (2.3). Again, one asks if the electron velocity as computed from the first moment of (3.1) is compatible with the corresponding expression arising from (2.3). A positive answer can be found by following a similar procedure as in the previous section. First, one replaces (1.5) in (3.1) and then one takes the first moment of the resulting kinetic equation. As a result, one obtains

$$\begin{aligned}
&\frac{\partial}{\partial t}(\boldsymbol{K}_e - n_e\boldsymbol{V}_e) + \boldsymbol{V}_e \boldsymbol{\cdot} \nabla (\boldsymbol{K}_e - n_e\boldsymbol{V}_e) + \nabla \boldsymbol{\cdot} (\boldsymbol{V}_e\boldsymbol{K}_e - n_e\boldsymbol{V}_e\boldsymbol{V}_e) \\
&\quad = (\boldsymbol{K}_e - n_e\boldsymbol{V}_e) \times \left(\boldsymbol{\omega}_e - \frac{e}{m_e}\boldsymbol{B}\right),
\end{aligned} \tag{4.5}$$

where we recall that $\boldsymbol{\omega}_e = \nabla \times \boldsymbol{V}_e$ is the electron vorticity and $(n_e, \boldsymbol{V}_e)$ are expressed by using (2.3). Then, we conclude that if $\boldsymbol{K}_e = n_e\boldsymbol{V}_e$ is verified initially, then it stays so at all times.

As a further remark on the neutral Vlasov model, we notice that Ohm's law (1.1) is not suitable for the numerical implementation, since the electron mean-flow inertia produces an explicit time derivative in the expression of the electric field. In his thesis, Burby expanded (1.1) by using (2.3) to obtain (1.7) in the form

$$\left(1+\frac{Zm_e}{m_i}\right)\boldsymbol{E}+\frac{m_e}{\mu_0 e^2 n_e}\nabla\times\nabla\times\boldsymbol{E}=-\left(1+\frac{Zm_e}{m_i}\right)\boldsymbol{V}_i\times\boldsymbol{B} \\ +\frac{1}{en_e}\left[\boldsymbol{J}\times\boldsymbol{B}-\nabla\boldsymbol{\cdot}\left(\widetilde{\mathbb{P}}_e-\frac{Zm_e}{m_i}\widetilde{\mathbb{P}}_i\right)\right]+\frac{m_e}{e^2n_e}\left[\nabla\boldsymbol{\cdot}\left(\boldsymbol{V}_i\boldsymbol{J}+\boldsymbol{J}\boldsymbol{V}_i-\frac{\boldsymbol{J}\boldsymbol{J}}{en_e}\right)\right], \tag{4.6}$$

with $\boldsymbol{J}=\mu_0^{-1}\nabla\times\boldsymbol{B}$. While on one hand this eliminates the time derivative in the closure for the electric field, one the other hand it involves inverting the operator $\psi+\mathrm{curl}^2$ for some function $\psi(\boldsymbol{x})$. (Here we shall not dwell upon the question of the numerical costs involved in inverting this operator). We remark that here we did not set $\nabla\boldsymbol{\cdot}\boldsymbol{E}$ to zero, as there is absolutely no reason for this to hold: indeed, quasi-neutrality is obtained by letting $\epsilon_0\to 0$ in Gauss' law, while no hypothesis is made on $\nabla\boldsymbol{\cdot}\boldsymbol{E}$.

The linear stability of the neutral Vlasov model can be easily studied since, as already noticed in Tronci & Camporeale (2015) it suffices to take the limit $\epsilon_0\to 0$ in the standard dispersion relation for the Vlasov–Maxwell system. Then, for example, the case of the Weibel instability can be studied by simply discarding the term ω^2/ω_{pe}^2 in (2.11) so that

$$1+\frac{T_\perp^{(e)}}{T_\parallel^{(e)}}W\left(\frac{\omega}{kv_{e\parallel}}\right)=-k^2\delta_e^2-Z\bar{\mu}\frac{T_\perp^{(i)}}{T_\parallel^{(i)}}\left[1+W\left(\frac{\omega}{kv_{i\parallel}}\right)\right]. \tag{4.7}$$

In the next section we show the results obtained with the neutral Vlasov model for both the electron and the ion Weibel instabilities.

4.3. *Discussion on quasi-neutral kinetic models*

This section compares the dispersion relations for the ion and electron Weibel instability derived from the CJ and the neutral Vlasov model. As it was done in previous sections, the case of the electron Weibel instability is studied by adopting a cold-fluid closure for ion kinetics. Thus, upon setting $T_\perp^{(i)}=T_\parallel^{(i)}$ and $W(\omega/kv_{i\parallel})\simeq 0$, equations (4.2) and (4.7) become

$$1+\frac{T_\perp^{(e)}}{T_\parallel^{(e)}}W\left(\frac{\omega}{kv_{e\parallel}}\right)=-k^2\delta_e^2 \tag{4.8}$$

and

$$1+\frac{T_\perp^{(e)}}{T_\parallel^{(e)}}W\left(\frac{\omega}{kv_{e\parallel}}\right)=-k^2\delta_e^2-Z\bar{\mu}, \tag{4.9}$$

respectively. We notice how the electron kinetics completely decouples from the ions in (4.8), while a minor coupling persists in (4.9). Similarly, the case of the ion Weibel instability can now be studied by adopting a cold-fluid closure for electron kinetics (not available in previous sections, which instead adopted an electron warm-fluid closure for the ion Weibel instability). In this case, setting $T_\perp^{(e)}=T_\parallel^{(e)}$ and $W(\omega/kv_{e\parallel})\simeq 0$ in (4.2) and (4.7) leads to

$$Z\bar{\mu}\frac{T_\perp^{(i)}}{T_\parallel^{(i)}}W\left(\frac{\omega}{kv_{i\parallel}}\right)=-1-k^2\delta_e^2 \tag{4.10}$$

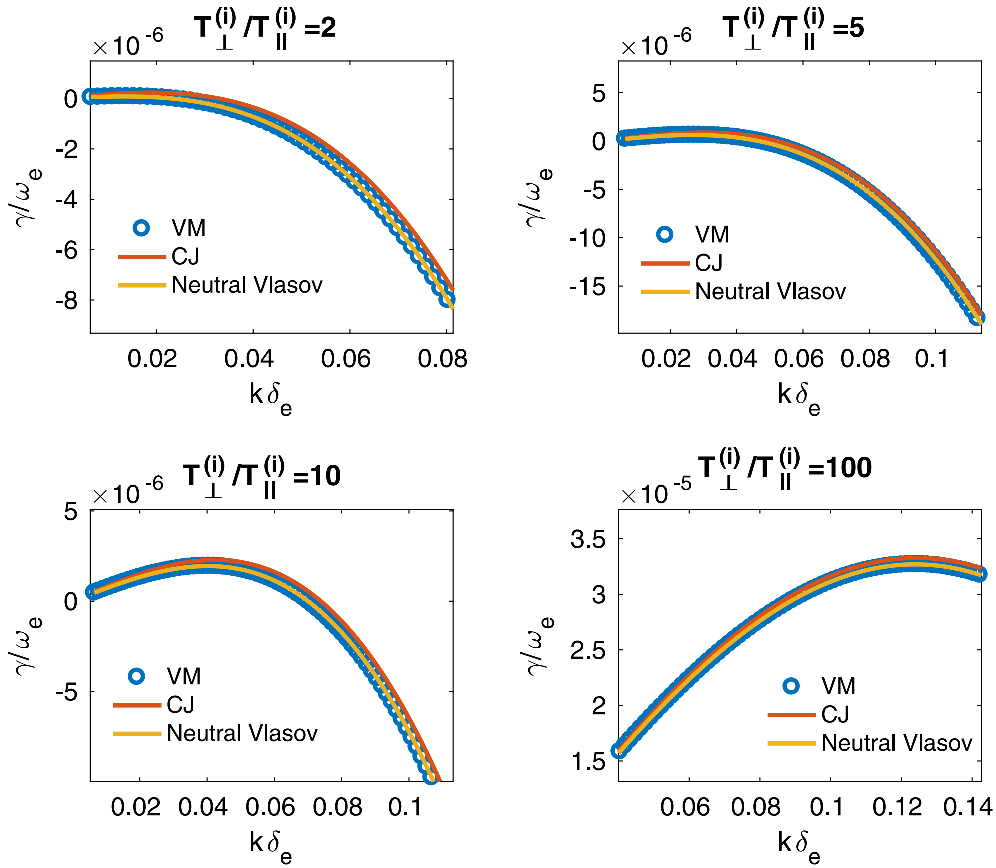

FIGURE 6. Growth rate for the ion Weibel instability for four values of temperature anisotropy $T_\perp/T_\parallel = 2, 5, 10, 100$. The blue circles are the reference solutions derived from the Vlasov–Maxwell model, the red lines are the solution of the CJ model, the blue lines are for the neutral Vlasov model.

and

$$Z\bar{\mu}\frac{T_\perp^{(i)}}{T_\parallel^{(i)}} W\left(\frac{\omega}{kv_{i\parallel}}\right) = -1 - k^2\delta_e^2 - Z\bar{\mu}\frac{T_\perp^{(i)}}{T_\parallel^{(i)}}, \tag{4.11}$$

respectively. We notice that certain differences between the two models may be appreciated in this case only for unusual anisotropy values of the order of $T_\perp^{(i)}/T_\parallel^{(i)} \simeq \bar{\mu}^{-1}$.

The dispersion relations (4.10)–(4.11) and (4.8)–(4.9) for the ion and electron Weibel instability derived from the CJ and the neutral Vlasov model are presented in figures 6 and 7, respectively. The results for the electron instability are indistinguishable from the VM solutions (obtained upon suitably specializing (2.11) for the case of electron and ion Weibel instabilities). Neutral Vlasov solutions are not shown as they also overlap with the VM solutions. For what concerns the ion instability a very small discrepancy can be noticed between the VM and the CJ, with the latter typically overestimating the growth/damping rates. However, the values are very small.

https://doi.org/10.1017/S0022377817000381 Published online by Cambridge University Press

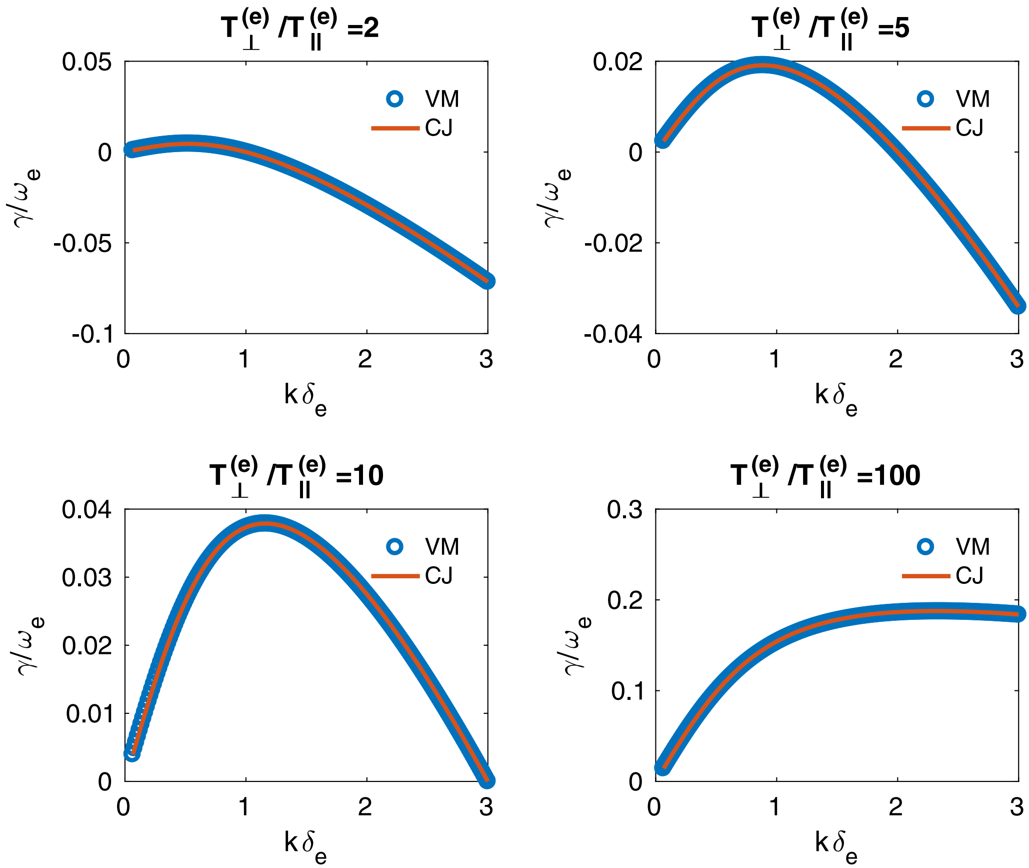

FIGURE 7. Growth rate for the electron Weibel instability for four values of temperature anisotropy $T_{\perp}/T_{\|}=2, 5, 10, 100$. The blue circles are the reference solutions derived from the Vlasov–Maxwell model, while the red lines are the solution of the CJ model. The neutral Vlasov solution coincides with both the VM and CJ solutions.

5. Conclusions and perspectives

The development and study of reduced models is a central theme in plasma physics, where the large separation of time and space scales between different species often makes computationally infeasible to tackle the first-principle dynamics (see, e.g. Camporeale & Burgess 2016). In this paper, we have addressed the problem of using reduced forms of Ohm's law to couple electrons and ions species. We have studied the validity of different approximation schemes by studying the linear dispersion relation for both electron and ion Weibel instabilities. In a sense, this is the simplest, yet not trivial, electromagnetic instability that one would like to be able to recover in an unmagnetized plasma. The Weibel instability has important physical implications for magnetic field generation in astrophysical and cosmological scenarios (Fonseca *et al.* 2003; Schlickeiser & Shukla 2003).

In § 2.1, we have studied a moment model, initially introduced by Hesse and Winske and later developed further by Kuztnetsova. This model was then extended to a fully kinetic theory that neglects electron inertia, in § 3.1. Also, § 4.1 discussed a quasi-neutral kinetic model introduced by Cheng and Johnson, who neglected terms of

https://doi.org/10.1017/S0022377817000381 Published online by Cambridge University Press

the order of the mass ratio. Furthermore for each one of the above mentioned model, we have studied similar variants introduced through variational methods, where the approximations are introduced at the level of Hamilton's principle. In particular, the quasi-neutral Vlasov model (simply named *neutral Vlasov*) was introduced by the authors in Tronci & Camporeale (2015).

Among the available reduced models, we have shown that only the quasi-neutral models (with electron inertia) are able to reproduce correctly the dispersion relation for the Weibel instability for both cases of ion and electron temperature anisotropy, thereby highlighting the importance of a kinetic derivation of the electron pressure tensor. The most important difference between the CJ and the neutral Vlasov models is that the latter preserves Ampère's current balance. This ensures the equality, at all times, between the mean velocity calculated through the first moment of the distribution function, and the same quantity calculated through Ampere's law (2.3). In turn, this also guarantees charge conservation and thus quasi-neutrality.

Acknowledgements

This paper belongs to the special issue for the conference Vlasovia 2016, held in Copanello (Italy); we thank all the participants interested in this work for inspiring discussions. Also, we are grateful to J. W. Burby, E. Cazzola, M. E. Innocenti, G. Lapenta, G. Manfredi, P. J. Morrison and F. Pegoraro for stimulating conversations on this and related topics. C.T. acknowledges financial support by the Leverhulme Trust Research Project Grant no. 2014-112, and by the London Mathematical Society Grant no. 31633 (Applied Geometric Mechanics Network).

Appendix A

A.1. *The dispersion relation for moment models*

In this appendix, we derive the dispersion relations (2.5) and (2.9) for the moment models treated in § 2.

First, we decompose all quantities as $X = X_0 + X_1$ (where the subscripts 0 and 1 denote the equilibrium configuration and its perturbation, respectively). Then, we linearize the ion Vlasov equation to find

$$\frac{\partial f_1}{\partial t} + \boldsymbol{v}\boldsymbol{\cdot}\frac{\partial f_1}{\partial \boldsymbol{x}} + \left[\frac{e}{m_e}\left(\frac{\partial \boldsymbol{A}_1}{\partial t} + \nabla\varphi_1 - \boldsymbol{v}\times\boldsymbol{B}_1\right)\right]\boldsymbol{\cdot}\frac{\partial f_0}{\partial \boldsymbol{v}} = 0, \tag{A 1}$$

where we have dropped the subscript i for convenience of notation. Upon applying the method of characteristics (Krall & Trivelpiece 1973), we write $X_1 = \widetilde{X}_1 \mathrm{e}^{kz-\omega t}$ and find

$$\begin{aligned}\tilde{f}_1 &= -i\frac{Ze}{m_i}\int_{-\infty}^{0}\left(\omega\widetilde{\boldsymbol{A}}_1 - \widetilde{\varphi}_1\boldsymbol{k} + \boldsymbol{v}\times\boldsymbol{k}\times\widetilde{\boldsymbol{A}}_1\right)\boldsymbol{\cdot}\frac{\partial f_0}{\partial \boldsymbol{v}}\mathrm{e}^{\mathrm{i}(kv_z-\omega)\tau}\,\mathrm{d}\tau \\ &= \frac{Ze}{m_i}\left[\widetilde{\boldsymbol{A}}_1 + \frac{\widetilde{\varphi}_1 - \boldsymbol{v}\boldsymbol{\cdot}\widetilde{\boldsymbol{A}}_1}{kv_z-\omega}\boldsymbol{k}\right]\boldsymbol{\cdot}\frac{\partial f_0}{\partial \boldsymbol{v}}.\end{aligned} \tag{A 2}$$

At this point, we denote by $\boldsymbol{K}_i = \int \boldsymbol{v}f_i\,\mathrm{d}\boldsymbol{v}$ the momentum of the ion mean flow and we compute its planar projection (by dropping the subscript i) as

$$\widetilde{\boldsymbol{K}}_{1\perp} = \frac{Ze}{m_i}\int \boldsymbol{v}_\perp\left(\widetilde{\boldsymbol{A}}_{1\perp}\boldsymbol{\cdot}\frac{\partial f_0}{\partial \boldsymbol{v}_\perp}\right) - \frac{Ze}{m_i}\int k\boldsymbol{v}_\perp\frac{\boldsymbol{v}_\perp\boldsymbol{\cdot}\widetilde{\boldsymbol{A}}_{1\perp}}{kv_z-\omega}\frac{\partial f_0}{\partial v_z}$$

https://doi.org/10.1017/S0022377817000381 Published online by Cambridge University Press

$$= -\frac{e}{m_i} n_0 \widetilde{\boldsymbol{A}}_{1\perp} - \frac{Ze}{m_i} \widetilde{\boldsymbol{A}}_{1\perp} \int \frac{1}{2} \frac{k v_\perp^2}{k v_z - \omega} \frac{\partial f_0}{\partial v_z} \tag{A 3}$$

$$= -\frac{e}{m_i} n_0 \left[1 + \frac{T_\perp^{(i)}}{T_\parallel^{(i)}} W\left(\frac{\omega}{k v_{i\parallel}} \right) \right] \widetilde{\boldsymbol{A}}_{1\perp}, \tag{A 4}$$

where we have used the fact that $f_0 = f_0(v_\perp^2, v_z^2)$ (notice, f_0 is an even function of $v_\perp$) and so $\int \boldsymbol{v}_\perp \boldsymbol{v}_\perp f_0 \, \mathrm{d}\boldsymbol{v}_\perp = (\int (v_\perp^2/2) f_0 \, \mathrm{d}\boldsymbol{v}_\perp)\mathbf{1}$ (here, $\mathbf{1}$ denotes the identity matrix). Also, here we have introduced the superscript (i) on the ion temperatures as well as the notation

$$W(\xi) = -1 - \xi \mathcal{Z}(\xi), \tag{A 5}$$

where $\mathcal{Z}$ denotes the plasma dispersion function. In addition, here $v_{i\parallel}$ denotes the ion thermal velocity in the parallel direction. As a subsequent step, we linearize Ampère's law $Ze\boldsymbol{K}_i - en_e\boldsymbol{V}_e = \mu_0^{-1} \nabla \times \boldsymbol{B}$ to obtain

$$\widetilde{\boldsymbol{K}}_{1\perp} = \frac{n_0}{Z} \left(\widetilde{\boldsymbol{V}}_{1\perp} + \frac{e}{m_e} k^2 \delta_e^2 \widetilde{\boldsymbol{A}}_{1\perp} \right) \tag{A 6}$$

so that eventually

$$-\frac{e}{m_i} n_0 \left[1 + \frac{T_\perp^{(i)}}{T_\parallel^{(i)}} W\left(\frac{\omega}{k v_{i\parallel}} \right) \right] \widetilde{\boldsymbol{A}}_{1\perp} = \frac{n_0}{Z} \left(\widetilde{\boldsymbol{V}}_{1\perp} + \frac{e}{m_e} k^2 \delta_e^2 \widetilde{\boldsymbol{A}}_{1\perp} \right) \tag{A 7}$$

and thus

$$\widetilde{\boldsymbol{V}}_{1\perp} = -\left\{ \frac{e}{m_e} k^2 \delta_e^2 + \frac{Ze}{m_i} \left[1 + \frac{T_\perp^{(i)}}{T_\parallel^{(i)}} W\left(\frac{\omega}{k v_{i\parallel}} \right) \right] \right\} \widetilde{\boldsymbol{A}}_{1\perp}. \tag{A 8}$$

At this point, we linearize the electron pressure equation to obtain

$$\begin{aligned} &\omega \widetilde{\mathbb{P}}_1 - \widetilde{\boldsymbol{V}}_1 (\boldsymbol{k} \cdot \mathbb{P}_0) - (\boldsymbol{k} \cdot \widetilde{\boldsymbol{V}}_1) \mathbb{P}_0 - (\boldsymbol{k} \cdot \mathbb{P}_0) \widetilde{\boldsymbol{V}}_1 \\ &\quad - \alpha (\mathbb{P}_0 \times (\boldsymbol{k} \times \widetilde{\boldsymbol{V}}_1) - (\boldsymbol{k} \times \widetilde{\boldsymbol{V}}_1) \times \mathbb{P}_0) + i \frac{e}{m_e} (\mathbb{P}_0 \times \widetilde{\boldsymbol{B}}_1 - \widetilde{\boldsymbol{B}}_1 \times \mathbb{P}_0) = 0. \end{aligned} \tag{A 9}$$

Notice that we have included the Coriolis force terms for completeness; when $\alpha = 0$, the equation above returns the HW model, while $\alpha = 1$ retains the Coriolis force consistently. Then, we take the dot product of the equation above with $\boldsymbol{k}$ (strictly speaking, we contract the pressure tensor equation with the vector $\boldsymbol{k}$). To this purpose, we compute

$$(\boldsymbol{k} \cdot \mathbb{P}_0) \times (\boldsymbol{k} \times \widetilde{\boldsymbol{V}}_1) = (\boldsymbol{k} \widetilde{\boldsymbol{V}}_1 : \mathbb{P}_0) \boldsymbol{k} - (\boldsymbol{k}\boldsymbol{k} : \mathbb{P}_0) \widetilde{\boldsymbol{V}}_1 \tag{A 10}$$

$$\begin{aligned} \boldsymbol{k} \cdot ((\boldsymbol{k} \times \widetilde{\boldsymbol{V}}_1) \times \mathbb{P}_0) &= \boldsymbol{k} \cdot \int ((\boldsymbol{k} \times \widetilde{\boldsymbol{V}}_1) \times \boldsymbol{c}) \boldsymbol{c} f_0(\boldsymbol{c}) \, \mathrm{d}^3\boldsymbol{c} \\ &= -\boldsymbol{k} \cdot \int ((\boldsymbol{c} \cdot \widetilde{\boldsymbol{V}}_1) \boldsymbol{k} - (\boldsymbol{k} \cdot \boldsymbol{c}) \widetilde{\boldsymbol{V}}_1) \boldsymbol{c} f_0(\boldsymbol{c}) \, \mathrm{d}^3\boldsymbol{c} \\ &= -k^2 (\widetilde{\boldsymbol{V}}_1 \cdot \mathbb{P}_0) + (\boldsymbol{k} \cdot \widetilde{\boldsymbol{V}}_1) \mathbb{P}_0 \boldsymbol{k}, \end{aligned} \tag{A 11}$$

so that eventually

$$\omega \widetilde{\mathbb{P}}_1 \boldsymbol{k} = (1 - \alpha) p_\parallel (\boldsymbol{k} \cdot \widetilde{\boldsymbol{V}}_1) \boldsymbol{k} + (\alpha p_\perp + (1 - \alpha) p_\parallel) k^2 \widetilde{\boldsymbol{V}}_1 + i \frac{e}{m_e} (p_\perp - p_\parallel) \boldsymbol{k} \times \widetilde{\boldsymbol{B}}_1. \tag{A 12}$$

Taking the planar projection yields

$$\omega (\widetilde{\mathbb{P}}_1 \boldsymbol{k})_\perp = (\alpha p_\perp + (1 - \alpha) p_\parallel) k^2 \widetilde{\boldsymbol{V}}_{1\perp} + \frac{e}{m_e} (p_\perp - p_\parallel) k^2 \widetilde{\boldsymbol{A}}_{1\perp}. \tag{A 13}$$

https://doi.org/10.1017/S0022377817000381 Published online by Cambridge University Press

Now, we linearize Ohm's law (1.5) to write $en_0(\widetilde{\varphi}_1\boldsymbol{k}-\omega\widetilde{\boldsymbol{A}}_1)=\widetilde{\mathbb{P}}_1\boldsymbol{k}$. Taking the planar component of the latter equation yields

$$-en_0\omega^2\widetilde{\boldsymbol{A}}_{1\perp}=\omega(\widetilde{\mathbb{P}}_1\boldsymbol{k})_\perp \tag{A 14}$$

and by inserting the equations (A 8) and (A 13) we obtain

$$\begin{aligned}-en_0\omega^2\widetilde{\boldsymbol{A}}_{1\perp} &= \frac{e}{m_e}(p_\perp-p_\|)k^2\widetilde{\boldsymbol{A}}_{1\perp}-(\alpha p_\perp+(1-\alpha)p_\|)k^2\\ &\quad\times\left\{\frac{Ze}{m_i}\left[1+\frac{T_\perp^{(i)}}{T_\|^{(i)}}W\left(\frac{\omega}{kv_{i\|}}\right)\right]+\frac{e}{m_e}k^2\delta_e^2\right\}\widetilde{\boldsymbol{A}}_{1\perp}.\end{aligned} \tag{A 15}$$

Then, upon using the relation $m_en_0/p_\|=1/v_{e\|}$, the dispersion relation becomes

$$\frac{\omega^2}{k^2v_{e\|}^2}=1-\frac{T_\perp^{(e)}}{T_\|^{(e)}}+\left(\alpha\frac{T_\perp^{(e)}}{T_\|^{(e)}}+1-\alpha\right)\left\{\frac{Zm_e}{m_i}\left[1+\frac{T_\perp^{(i)}}{T_\|^{(i)}}W\left(\frac{\omega}{kv_{i\|}}\right)\right]+k^2\delta_e^2\right\}. \tag{A 16}$$

Then, the dispersion relation (2.5) for the HW model in the case of the Weibel instability is given by $\alpha=0$

$$\frac{\omega^2}{k^2v_{e\|}^2}=1-\frac{T_\perp^{(e)}}{T_\|^{(e)}}+\left\{\frac{Zm_e}{m_i}\left[1+\frac{T_\perp^{(i)}}{T_\|^{(i)}}W\left(\frac{\omega}{kv_{i\|}}\right)\right]+k^2\delta_e^2\right\}, \tag{A 17}$$

while retaining Coriolis effects (by setting $\alpha=1$) leads to (2.9), that is

$$\frac{\omega^2}{k^2v_{e\|}^2}=1-\frac{T_\perp^{(e)}}{T_\|^{(e)}}\left\{1-k^2\delta_e^2-\frac{Zm_e}{m_i}\left[1+\frac{T_\perp^{(i)}}{T_\|^{(i)}}W\left(\frac{\omega}{kv_{i\|}}\right)\right]\right\}. \tag{A 18}$$

A.2. *The dispersion relation for reduced kinetic models*

This appendix presents the dispersion relations (3.7) and (3.11) for the reduced models in §§ 3.1 and 3.2, in the case of the Weibel instability. The ion kinetic equation (2.2) was already linearized around the equilibrium

$$\boldsymbol{E}_0=\boldsymbol{B}_0=\boldsymbol{V}_{e0}=\boldsymbol{V}_{i0}=0,\quad f_0=f_0(v_\perp^2,v_z^2) \tag{A 19}$$

in § A.1, thereby leading to (A 2). In addition, in § A.1, linearizing Ampère's law led to (A 6) and to (A 8). At this point, we need to linearize electron kinetics around the equilibrium (3.6). To this purpose, we consider the following equation

$$\begin{aligned}&\frac{\partial \mathsf{f}_e}{\partial t}+(\boldsymbol{c}+\boldsymbol{V}_e)\boldsymbol{\cdot}\frac{\partial \mathsf{f}_e}{\partial \boldsymbol{x}}\\ &\quad-\left[\boldsymbol{c}\boldsymbol{\cdot}\nabla\boldsymbol{V}_e+\alpha\boldsymbol{c}\times\nabla\times\boldsymbol{V}_e-\frac{e}{m_e}\left(\frac{\partial\boldsymbol{A}}{\partial t}+\nabla\varphi-(\boldsymbol{c}+\boldsymbol{V}_e)\times\boldsymbol{B}\right)\right]\boldsymbol{\cdot}\frac{\partial \mathsf{f}_e}{\partial \boldsymbol{c}}=0,\end{aligned} \tag{A 20}$$

where $\alpha=0,1$ is a flag variable so that $\alpha=0$ corresponds to the kinetic HW system in § 3.1, while $\alpha=1$ corresponds to its variational variant in § 3.2. Upon linearizing around (3.6), we obtain

$$\frac{\partial \mathsf{f}_1}{\partial t}+\boldsymbol{c}\boldsymbol{\cdot}\frac{\partial \mathsf{f}_1}{\partial \boldsymbol{x}}-\left[\frac{q_e}{m_e}\left(\frac{\partial\boldsymbol{A}_1}{\partial t}+\nabla\varphi_1-\boldsymbol{c}\times\boldsymbol{B}_1\right)+\boldsymbol{c}\boldsymbol{\cdot}\nabla\boldsymbol{V}_1+\alpha\boldsymbol{c}\times\nabla\times\boldsymbol{V}_1\right]\boldsymbol{\cdot}\frac{\partial \mathsf{f}_0}{\partial \boldsymbol{c}}=0, \tag{A 21}$$

https://doi.org/10.1017/S0022377817000381 Published online by Cambridge University Press

where we have used the same notation as in § A.1. Again, upon using the method of characteristics and by Fourier transforming, we have

$$\begin{aligned}\widetilde{\mathsf{f}}_1 &= \int_{-\infty}^{0} [\zeta_e(\mathrm{i}\omega\widetilde{\boldsymbol{A}}_1 - \mathrm{i}\widetilde{\varphi}_1\boldsymbol{k} + \boldsymbol{c}\times\widetilde{\boldsymbol{B}}_1) + \mathrm{i}kc_z\widetilde{\boldsymbol{V}}_1 + \mathrm{i}\alpha\boldsymbol{c}\times\boldsymbol{k}\times\boldsymbol{V}_1]\boldsymbol{\cdot}\frac{\partial\mathsf{f}_0}{\partial\boldsymbol{c}}\mathrm{e}^{\mathrm{i}(kc_z-\omega)\tau}\,\mathrm{d}\tau \\ &= \mathrm{i}\int_{-\infty}^{0}\{\zeta_e(\omega-kc_z)\widetilde{\boldsymbol{A}}_1 - [\zeta_e\widetilde{\varphi}_1 - \boldsymbol{c}\boldsymbol{\cdot}(\zeta_e\widetilde{\boldsymbol{A}}_1+\alpha\widetilde{\boldsymbol{V}}_1)]\boldsymbol{k} + (1-\alpha)kc_z\widetilde{\boldsymbol{V}}_1\}\boldsymbol{\cdot}\frac{\partial\mathsf{f}_0}{\partial\boldsymbol{c}}\mathrm{e}^{\mathrm{i}(kc_z-\omega)\tau}\,\mathrm{d}\tau \\ &= -\left[\zeta_e\widetilde{\boldsymbol{A}}_1 + \frac{\zeta_e\widetilde{\varphi}_1 - \boldsymbol{c}\boldsymbol{\cdot}(\zeta_e\widetilde{\boldsymbol{A}}_1+\alpha\widetilde{\boldsymbol{V}}_1)}{kc_z-\omega}\boldsymbol{k} + \frac{(\alpha-1)kc_z}{kc_z-\omega}\widetilde{\boldsymbol{V}}_1\right]\boldsymbol{\cdot}\frac{\partial\mathsf{f}_0}{\partial\boldsymbol{c}},\end{aligned} \tag{A 22}$$

where we have introduced the notation $\zeta_e = e/m_e$. Therefore, the planar components of the pressure force term are

$$\begin{aligned} m_e^{-1}(\widetilde{\mathbb{P}}_1\boldsymbol{k})_\perp \\ = -\int kc_z\left\{\left[\zeta_e\widetilde{\boldsymbol{A}}_1 + \frac{\zeta_e\widetilde{\varphi}_1 - \boldsymbol{c}\boldsymbol{\cdot}(\zeta_e\widetilde{\boldsymbol{A}}_1+\alpha\widetilde{\boldsymbol{V}}_1)}{kc_z-\omega}\boldsymbol{k} + \frac{(\alpha-1)kc_z}{kc_z-\omega}\widetilde{\boldsymbol{V}}_1\right]\boldsymbol{\cdot}\frac{\partial\mathsf{f}_0}{\partial\boldsymbol{c}}\right\}\boldsymbol{c}_\perp\,\mathrm{d}^3\boldsymbol{c}.\end{aligned} \tag{A 23}$$

Then, we verify that

$$\int\left(kc_z\widetilde{\boldsymbol{A}}_1\boldsymbol{\cdot}\frac{\partial\mathsf{f}_0}{\partial\boldsymbol{c}}\right)\boldsymbol{c}_\perp\,\mathrm{d}^3\boldsymbol{c} = k\int\widetilde{\varphi}_1\frac{kc_z}{kc_z-\omega}\frac{\partial\mathsf{f}_0}{\partial c_z}\boldsymbol{c}_\perp\,\mathrm{d}^3\boldsymbol{c} = k^2\widetilde{A}_{1z}\int\frac{c_z^2}{kc_z-\omega}\frac{\partial\mathsf{f}_0}{\partial c_z}\boldsymbol{c}_\perp\,\mathrm{d}^3\boldsymbol{c} = 0 \tag{A 24}$$

and also

$$\int kc_z\left[\frac{kc_z(\alpha\widetilde{V}_{1z}+\zeta_e\widetilde{A}_{1z})}{kc_z-\omega} - \frac{(\alpha-1)kc_z}{kc_z-\omega}\widetilde{V}_{1z}\right]\frac{\partial\mathsf{f}_0}{\partial c_z}\boldsymbol{c}_\perp\,\mathrm{d}^3\boldsymbol{c} = 0. \tag{A 25}$$

With this in mind, and by recalling $\int\boldsymbol{v}_\perp\boldsymbol{v}_\perp\mathsf{f}_0\,\mathrm{d}\boldsymbol{v}_\perp = \left(\int(v_\perp^2/2)\mathsf{f}_0\,\mathrm{d}\boldsymbol{v}_\perp\right)\mathbf{1}$, we compute

$$\begin{aligned} m_e^{-1}(\widetilde{\mathbb{P}}_1\boldsymbol{k})_\perp &= \int kc_z\left\{\left[\frac{k\boldsymbol{c}_\perp\boldsymbol{\cdot}(\alpha\widetilde{\boldsymbol{V}}_{1\perp}+\zeta_e\widetilde{\boldsymbol{A}}_{1\perp})}{kc_z-\omega}\frac{\partial\mathsf{f}_0}{\partial c_z} - \frac{(\alpha-1)kc_z}{kc_z-\omega}\widetilde{\boldsymbol{V}}_{1\perp}\boldsymbol{\cdot}\frac{\partial\mathsf{f}_0}{\partial\boldsymbol{c}_\perp}\right]\right\}\boldsymbol{c}_\perp \\ &= \int kc_z\left[\frac{1}{2}\frac{kc_\perp^2\partial\mathsf{f}_0/\partial c_z}{kc_z-\omega}(\alpha\widetilde{\boldsymbol{V}}_{1\perp}+\zeta_e\widetilde{\boldsymbol{A}}_{1\perp}) + \frac{(\alpha-1)kc_z}{kc_z-\omega}\mathsf{f}_0\widetilde{\boldsymbol{V}}_{1\perp}\right] \\ &= n_0\omega\frac{T_\perp^{(e)}}{T_\parallel^{(e)}}(\alpha\widetilde{\boldsymbol{V}}_{1\perp}+\zeta_e\widetilde{\boldsymbol{A}}_{1\perp})\,W\left(\frac{\omega}{kv_{e\parallel}}\right) \\ &\quad + (\alpha-1)\omega\left[n_0 + \omega\int\frac{\mathsf{f}_0}{kc_z-\omega}\right]\widetilde{\boldsymbol{V}}_{1\perp} \\ &= n_0\omega\left[\frac{T_\perp^{(e)}}{T_\parallel^{(e)}}(\alpha\widetilde{\boldsymbol{V}}_{1\perp}+\zeta_e\widetilde{\boldsymbol{A}}_{1\perp}) + (1-\alpha)\widetilde{\boldsymbol{V}}_{1\perp}\right]W\left(\frac{\omega}{kv_{e\parallel}}\right).\end{aligned} \tag{A 26}$$

Now, the planar components of Ohm's law (as in (A 14)) yield

$$-\frac{e}{m_e}\left[1 + \frac{T_\perp^{(e)}}{T_\parallel^{(e)}}W\left(\frac{\omega}{kv_{e\parallel}}\right)\right]\widetilde{\boldsymbol{A}}_{1\perp} = \left[1 - \alpha\left(1 - \frac{T_\perp^{(e)}}{T_\parallel^{(e)}}\right)\right]W\left(\frac{\omega}{kv_{e\parallel}}\right)\widetilde{\boldsymbol{V}}_{1\perp}, \tag{A 27}$$

so that, upon recalling (A 8),

$$1+\frac{T_{\perp}^{(e)}}{T_{\parallel}^{(e)}}W\left(\frac{\omega}{kv_{e\parallel}}\right) = \left[1-\alpha\left(1-\frac{T_{\perp}^{(e)}}{T_{\parallel}^{(e)}}\right)\right] \times\left\{k^2\delta_e^2+Z\bar{\mu}\left[1+\frac{T_{\perp}^{(i)}}{T_{\parallel}^{(i)}}W\left(\frac{\omega}{kv_{i\parallel}}\right)\right]\right\}W\left(\frac{\omega}{kv_{e\parallel}}\right). \quad \text{(A 28)}$$

Then, the dispersion relation (3.7) for the HW kinetic model in the case of the Weibel instability is given by $\alpha=0$

$$1+\frac{T_{\perp}^{(e)}}{T_{\parallel}^{(e)}}W\left(\frac{\omega}{kv_{e\parallel}}\right)=\left\{k^2\delta_e^2+Z\bar{\mu}\left[1+\frac{T_{\perp}^{(i)}}{T_{\parallel}^{(i)}}W\left(\frac{\omega}{kv_{i\parallel}}\right)\right]\right\}W\left(\frac{\omega}{kv_{e\parallel}}\right), \quad \text{(A 29)}$$

while retaining Coriolis effects (by setting $\alpha=1$) leads to (3.11), that is

$$\frac{T_{\parallel}^{(e)}}{T_{\perp}^{(e)}}+W\left(\frac{\omega}{kv_{e\parallel}}\right)=\left\{k^2\delta_e^2+Z\bar{\mu}\left[1+\frac{T_{\perp}^{(i)}}{T_{\parallel}^{(i)}}W\left(\frac{\omega}{kv_{i\parallel}}\right)\right]\right\}W\left(\frac{\omega}{kv_{e\parallel}}\right). \quad \text{(A 30)}$$

A.3. *Dispersion relation for the Cheng–Johnson model*

This appendix presents the dispersion relation (4.2) that arises by linearizing the Cheng–Johnson model around the equilibrium (4.1). In this case, linearizing the form (1.8) of Ohm's law leads to

$$\frac{q_e^2}{m_e}n_0\boldsymbol{E}_1+\mu_0^{-1}\nabla\times\nabla\times\boldsymbol{E}_1=q_e\frac{1}{m_e}\nabla\cdot\mathbb{P}_{e\,1}+q_i\frac{1}{m_i}\nabla\cdot\mathbb{P}_{i\,1} \quad \text{(A 31)}$$

and taking the planar components after Fourier transforming leads to

$$\omega(1+k^2\delta^2)\widetilde{\boldsymbol{A}}_{1\perp}=\frac{1}{en_0}[(Z\bar{\mu}\,\widetilde{\mathbb{P}}_1^{(i)}-\widetilde{\mathbb{P}}_1^{(e)})\boldsymbol{k}]_{\perp}. \quad \text{(A 32)}$$

On the other hand, by adapting the result (A 26) to the present case, we have

$$m_s^{-1}(\widetilde{\mathbb{P}}_1^{(s)}\boldsymbol{k})_{\perp}=\pm\omega\frac{en_0}{m_s}\frac{T_{\perp}^{(s)}}{T_{\parallel}^{(s)}}W\left(\frac{\omega}{kv_{s\parallel}}\right)\widetilde{\boldsymbol{A}}_{1\perp}, \quad \text{(A 33)}$$

(where the plus is used when $s=e$ and the minus when $s=i$) and therefore we obtain (4.2) in the form

$$1+k^2\delta_e^2=-\frac{T_{\perp}^{(e)}}{T_{\parallel}^{(e)}}W\left(\frac{\omega}{kv_{e\parallel}}\right)-Z\bar{\mu}\frac{T_{\perp}^{(i)}}{T_{\parallel}^{(i)}}W\left(\frac{\omega}{kv_{i\parallel}}\right). \quad \text{(A 34)}$$

REFERENCES

AUNAI, N., HESSE, M. & KUZNETSOVA, M. 2013 Electron nongyrotropy in the context of collisionless magnetic reconnection. *Phys. Plasmas* **20** (9), 092903.

BASU, B. 2002 Moment equation description of weibel instability. *Phys. Plasmas* **9** (12), 5131–5134.

BIRN, J., DRAKE, J. F., SHAY, M. A., ROGERS, B. N., DENTON, R. E., HESSE, M., KUZNETSOVA, M., MA, Z. W., BHATTACHARJEE, A., OTTO, A. *et al.* 2001 Geospace environmental modeling (gem) magnetic reconnection challenge. *J. Geophys. Res.* **106** (A3), 3715–3719.

BRIZARD, A. J. 2000 New variational principle for the Vlasov–Maxwell equations. *Phys. Rev. Lett.* **84** (25), 5768.

BURBY, J. W. 2015 Chasing Hamiltonian structure in gyrokinetic theory. PhD thesis, Princeton University.

CAI, H.-J. & LEE, L. C. 1997 The generalized ohms law in collisionless magnetic reconnection. *Phys. Plasmas* **4** (3), 509–520.

CAMPOREALE, E. & BURGESS, D. 2016 Comparison of linear modes in kinetic plasma models. *J. Plasma Phys.* **83**, 535830201.

CAMPOREALE, E. & LAPENTA, G. 2005 Model of bifurcated current sheets in the earth's magnetotail: equilibrium and stability. *J. Geophys. Res.* **110**, A07206.

CAZZOLA, E., INNOCENTI, M. E., GOLDMAN, M. V., NEWMAN, D. L., MARKIDIS, S. & LAPENTA, G. 2016 On the electron agyrotropy during rapid asymmetric magnetic island coalescence in presence of a guide field. *Geophys. Res. Lett.* **43** (15), 7840–7849.

CENDRA, H., HOLM, D. D., HOYLE, M. J. W. & MARSDEN, J. E. 1998 The Vlasov–Maxwell equations in Euler–Poincaré form. *J. Math. Phys.* **39** (6), 3138–3157.

CHENG, C. Z. & JOHNSON, J. R. 1999 A kinetic-fluid model. *J. Geophys. Res.* **104** (A1), 413–427.

DEGOND, P., DELUZET, F. & DOYEN, D. 2017 Asymptotic-preserving particle-in-cell methods for the Vlasov–Maxwell system in the quasi-neutral limit. *J. Comput. Phys.* **330**, 467–492.

FONSECA, R. A., SILVA, L. O., TONGE, J. W., MORI, W. B. & DAWSON, J. M. 2003 Three-dimensional weibel instability in astrophysical scenarios. *Phys. Plasmas* **10** (5), 1979–1984.

GARY, S. P. & KARIMABADI, H. 2006 Linear theory of electron temperature anisotropy instabilities: whistler, mirror, and weibel. *J. Geophys. Res.* **111**, A11224.

GHIZZO, A., SARRAT, M. & DEL SARTO, D. 2017 Vlasov models for kinetic weibel-type instabilities. *J. Plasma Phys.* **83**, 705830101.

GRAD, H. 1949 On the kinetic theory of rarefied gases. *Commun. Appl. Maths* **2** (4), 331–407.

HAYNES, C. T., BURGESS, D. & CAMPOREALE, E. 2014 Reconnection and electron temperature anisotropy in sub-proton scale plasma turbulence. *Astrophys. J.* **783** (1), 38.

HESSE, M., KUZNETSOVA, M. & BIRN, J. 2004 The role of electron heat flux in guide-field magnetic reconnection. *Phys. Plasmas* **11** (12), 5387–5397.

HESSE, M. & WINSKE, D. 1993 Hybrid simulations of collisionless ion tearing. *Geophys. Res. Lett.* **20** (12), 1207–1210.

HESSE, M. & WINSKE, D. 1994 Hybrid simulations of collisionless reconnection in current sheets. *J. Geophys. Res.* **99** (A6), 11177–11192.

HOLM, D. D. & TRONCI, C. 2012 Euler-poincare formulation of hybrid plasma models. *Commun. Math. Sci.* **10**, 191–222; (EPFL-ARTICLE-174831).

KRALL, N. A. & TRIVELPIECE, A. W. 1973 *Principles of Plasma Physics*. McGraw Hill.

KUZNETSOVA, M. M., HESSE, M. & WINSKE, D. 1998 Kinetic quasi-viscous and bulk flow inertia effects in collisionless magnetotail reconnection. *J. Geophys. Res.* **103** (A1), 199–213.

KUZNETSOVA, M. M., HESSE, M. & WINSKE, D. 2000 Toward a transport model of collisionless magnetic reconnection. *J. Geophys. Res.* **105** (A4), 7601–7616.

LITTLEJOHN, R. G. 1983 Variational principles of guiding centre motion. *J. Plasma Phys.* **29** (01), 111–125.

LOW, F. E. 1958 A Lagrangian formulation of the Boltzmann–Vlasov equation for plasmas. *Proc. R. Soc. Lond.* A **248**, 282–287; The Royal Society.

MORRISON, P. J. 1998 Hamiltonian description of the ideal fluid. *Rev. Mod. Phys.* **70** (2), 467.

NEWCOMB, W. A. 1962 Lagrangian and Hamiltonian methods in magnetohydrodynamics. *Nucl. Fusion* 451–463.

SARRAT, M., DEL SARTO, D. & GHIZZO, A. 2016 Fluid description of weibel-type instabilities via full pressure tensor dynamics. *Europhys. Lett.* **115** (4), 45001.

SCHLICKEISER, R. & SHUKLA, P. K. 2003 Cosmological magnetic field generation by the weibel instability. *Astrophys. J. Lett.* **599** (2), L57.

SWISDAK, M. 2016 Quantifying gyrotropy in magnetic reconnection. *Geophys. Res. Lett.* **43** (1), 43–49.

THYAGARAJA, A. & MCCLEMENTS, K. G. 2009 Plasma physics in noninertial frames. *Phys. Plasmas* **16** (9), 092506.

TRONCI, C. 2013 A Lagrangian kinetic model for collisionless magnetic reconnection. *Plasma Phys. Control. Fusion* **55** (3), 035001.

TRONCI, C. & CAMPOREALE, E. 2015 Neutral Vlasov kinetic theory of magnetized plasmas. *Phys. Plasmas* **22** (2), 020704.

WANG, L., HAKIM, A. H., BHATTACHARJEE, A. & GERMASCHEWSKI, K. 2015 Comparison of multi-fluid moment models with particle-in-cell simulations of collisionless magnetic reconnection. *Phys. Plasmas* **22** (1), 012108.

WANG, X., BHATTACHARJEE, A. & MA, Z. W. 2000 Collisionless reconnection: effects of hall current and electron pressure gradient. *J. Geophys. Res.* **105** (A12), 27633–27648.

WEIBEL, E. S. 1959 Spontaneously growing transverse waves in a plasma due to an anisotropic velocity distribution. *Phys. Rev. Lett.* **2** (3), 83.

WINSKE, D. & HESSE, M. 1994 Hybrid modeling of magnetic reconnection in space plasmas. *Physica* D **77** (1–3), 268–275.

YIN, L. & WINSKE, D. 2003 Plasma pressure tensor effects on reconnection: hybrid and hall-magnetohydrodynamics simulations. *Phys. Plasmas* **10** (5), 1595–1604.

YIN, L., WINSKE, D., GARY, S. P. & BIRN, J. 2001 Hybrid and hall-mhd simulations of collisionless reconnection: dynamics of the electron pressure tensor. *J. Geophys. Res.* **106** (A6), 10761–10775.